Tumor growth at the primary site and body weight were continuously monitored. Intratumoral injection of OBP-301 in both regimens induced a gradual reduction in tumor volumes compared with mock-treated mice. Mice with tumor shrinkage significantly recovered body weight starting on day 10 (regimen 1) or day 15 (regimen 2) after the last virus injection ($P < 0.05$), although there was a decrease in body weight in the control group (Fig. 3D). This antitumor effect could be observed in mice orthotopically implanted with HSC-3 cells; the appearance of the effect, however, was ~4 to 5 days slower than that of SAS-L tumor-bearing mice (Supplementary Fig. S4).

Locoregional spread of virus following virotherapy in an orthotopic human SCCHN model. SCCHN patients with metastases to regional lymph nodes have a poorer prognosis than patients without nodal metastases (16). To verify whether adenoviruses could traffic to regional lymph nodes through the lymphatics, we injected 1×10^8 pfu of OBP-401 into SAS-L tumors implanted into the tongues of mice. Five days after virus injection, primary tongue tumors as well as lymph node metastases could be detected as light-emitting spots with GFP fluorescence under the optical charge-coupled device imaging (Fig. 5A). We also found that OBP-401 could infect and replicate in SAS-L cells trafficking in lymphatic vessels (Fig. 5B). These results suggest that although adenoviruses could effectively drain to regional lymph nodes, OBP-401 replicated only in metastatic lymph nodes, which was confirmed by a histopathologic analysis. Metastatic SCCHN cells were mostly observed in the lymph nodes with fluorescence emission, whereas most of GFP-negative lymph nodes contained no tumor cells (Fig. 5C). The optical imaging detected 13 lymph nodes labeled in spots with GFP fluorescence in 14 metastatic nodes (sensitivity of 92.9%). Among 21 metastasis-free lymph nodes, 3 nodes were GFP positive (specificity of 85.7%). In another orthotopic model implanted with HSC-3 human SCCHN cells, we could also detect GFP signals in one or two metastatic lymph nodes but not in other nonmetastatic nodes and salivary glands (Fig. 5; Supplementary Fig. S5).

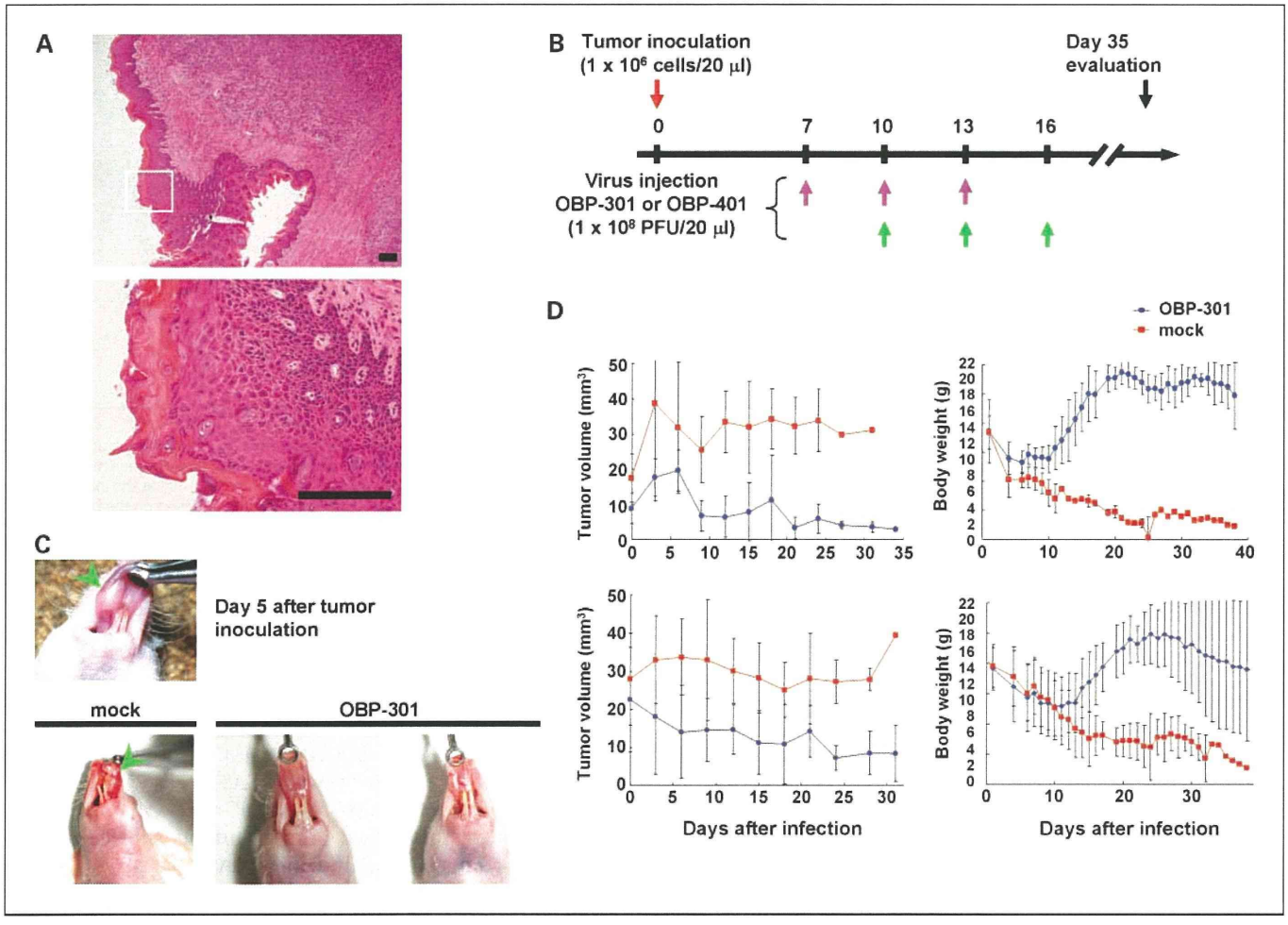

Fig. 3. Antitumor effects of OBP-301 *in vivo* in an orthotopic SCCHN model. *A,* tumor sections were obtained 35 d after tumor cell implantation. Paraffin-embedded sections of SAS-L tongue tumors were stained with H&E. Scale bar, 100 μm. Top, ×40 magnification; bottom, detail of the boxed region of the top panel; magnification, ×400. *B,* orthotopic animal experiment regimens. The tongues of BALB/c *nu/nu* mice were inoculated with 1×10^5 SAS-L human SCCHN cells. Orthotopic tumor-bearing mice received three courses of intratumoral injection of 1×10^8 pfu of viruses every 3 d starting on day 7 (regimen 1) or day 10 (regimen 2) after tumor cell inoculation. Eight mice were used in each group. *C,* macroscopic appearance of SAS-L tongue tumors on BALB/c *nu/nu* mice 5 d (*top*) or 35 d (*bottom*) after tumor cell inoculation. Representative tumors treated with PBS or OBP-301 are shown. Note the eradicated tumors in mice that received OBP-301 injection. Green arrowhead, SAS-L tumors. *D,* orthotopic tumor-bearing mice received three courses of intratumoral injection of 1×10^8 pfu of viruses every 3 d starting on day 7 (regimen 1; *top*) or day 10 (regimen 2; *bottom*) after tumor cell inoculation. The tumor volume (*left*) and the body weight (*right*) were monitored and plotted. Point, mean; bars, SD. Statistical significance was defined as $P < 0.05$.

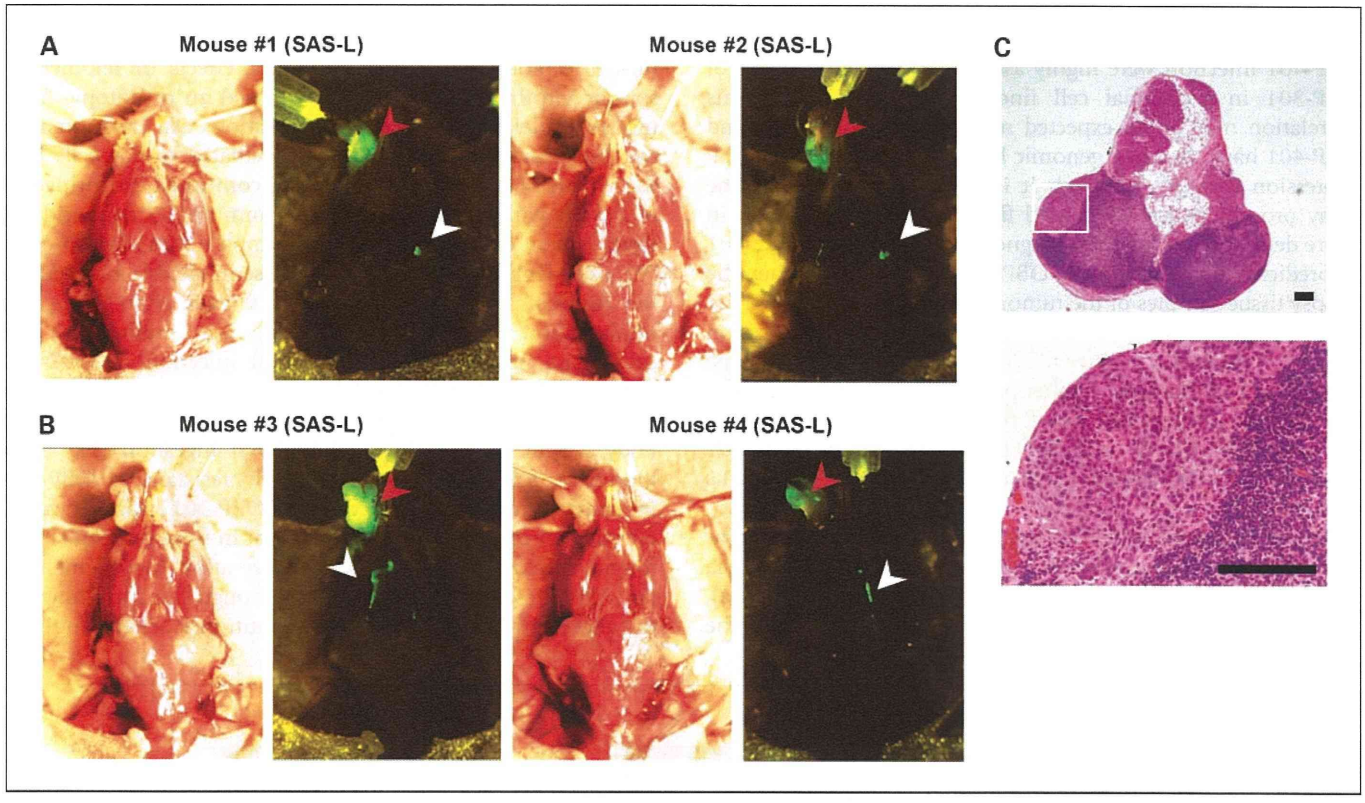

Fig. 4. Virus spread of OBP-401 via lymphatics to regional lymph nodes on SAS-L tumor-bearing mice. *A,* selective visualization of lymph node metastasis in orthotopic xenografts of SAS-L human SCCHN cells. Mice received intratumoral injection of OBP-401 (1×10^8 pfu) 24 d after tumor inoculation and were assessed for lymph node metastasis 5 d later under charge-coupled device imaging. Left, gross appearance; right, fluorescence image. Red arrowhead, primary tumor; white arrowhead, metastatic tumor cells. *B,* selective visualization of lymph node metastasis and lymphatic dissemination in orthotopic xenografts of SAS-L cells. Note the GFP-expressing disseminated tumor cells in lymphatics. Red arrowhead, primary tumor; white arrowhead, metastatic tumor cells in lymphatics. *C,* sections of GFP-positive lymph nodes were obtained 35 d after tumor cell implantation. Paraffin-embedded sections of lymph nodes were stained with H&E. Scale bar, 100 μm.

Prolonged survival following OBP-301 virotherapy in an orthotopic human SCCHN model. Finally, we assessed the effect of intratumoral injection of OBP-301 on survival time of SAS-L–bearing mice. Mice treated with OBP-301 beginning either on the 7th day (regimen 1) or the 10th day (regimen 2) after tumor implantation survived significantly longer (mean = 27.4 or 33.7 days) than mice without treatment (mean = 14.7 or 24.3 days; regimen 1, $P = 0.017$; regimen 2, $P = 0.016$; Fig. 6). The prolonged survival might reflect an antitumor effect of oncolytic adenoviruses spreading into the locoregional area, including regional lymph nodes.

Discussion

The present study illustrates the potential application of replication-selective oncolytic adenoviruses as an anticancer agent in human SCCHN patients. We found that intratumoral administration of telomerase-specific oncolytic adenovirus induced tumor volume reduction as well as the recovery of weight loss by enabling oral ingestion in an orthotopic xenograft model, in which human SCCHN cells were implanted into the tongues of BALB/c *nu/nu* mice. Oncolytic virotherapy also prolonged the survival of SCCHN tumor-bearing mice, presumably due to the locoregional antitumor effect against primary tumors and lymph node metastases with viruses spreading into the lymphatics.

Telomerase-specific oncolytic adenovirus OBP-301 exhibits a broad cytopathic effect against human cancer cell lines of different tissue origins (8–10). In a panel of human SCCHN cell lines, OBP-301 also showed apparent antitumor effects *in vitro* in a dose-dependent manner (Fig. 1B), although the sensitivity varied greatly between cell lines despite hTERT and coxsackievirus and adenovirus receptor expression (Supplementary Fig. S1). We have previously found that the process of oncolysis is morphologically distinct from apoptosis and necrosis (17). The cell death machinery triggered by OBP-301 infection is still under the investigation, although autophagy is partially involved in this effect (17, 18). OBP-301 has been developed based on the ability of the hTERT promoter to control replication of the virus in the tumors, leading to selective killing of tumor cells and minimal undesired effects on normal cells; the ID_{50} values of OBP-301 in various human cancer cell lines, however, were not related to the levels of *hTERT* mRNA expression (8, 10). Indeed, HSC-3 and HSC-4 human SCCHN cells expressing high levels of *hTERT* mRNA were less sensitive to OBP-301 than SCC-4 and SCC-9 cells with low levels of hTERT expression. Thus, neither hTERT expression nor coxsackievirus and adenovirus receptor expression could be useful for predicting the outcome of OBP-301 treatment.

Biomarkers have been extensively studied and often used to predict the potential therapeutic benefit of new agents, including molecular-targeted therapies (19). There is a widely recognized need for biomarkers that could improve the

clinician's ability to select suitable drugs for appropriate patients. We found that the levels of GFP expression following OBP-401 infection were highly associated with ID_{50} values of OBP-301 in individual cell lines *in vitro* (Fig. 2C). This correlation may be an expected result, because OBP-301 and OBP-401 have the same genomic backbone except for the GFP expression cassette. Although it is necessary to establish the assay procedures for GFP-based fluorescence measurement in more detail, we propose the diagnostic application of OBP-401 to predict tumor responses to OBP-301. For example, when the biopsy tissue samples of the tumor are exposed to OBP-401 for a certain amount of time *ex vivo*, the levels of GFP expression may be of value as a positive predictive marker for the outcome of OBP-301 virotherapy. Further prospective clinical studies are required to confirm the direct correlation between the GFP expression in biopsy samples following *ex vivo* OBP-401 infection and the clinical responses to OBP-301 in patients with SCCHN.

An orthotopic nude mouse model to investigate the cellular and molecular mechanisms of metastasis in human neoplasia was first described by Fidler et al. (20, 21) and Killion et al. (22). The orthotopic implantation of tumor cells restores the correct tumor-host interactions, which do not occur when tumors are implanted in ectopic subcutaneous sites (20). To further explore the *in vivo* antitumor effects of telomerase-specific virotherapy for SCCHN, we used an orthotopic nude mouse model of human tongue squamous cell carcinoma. In our preliminary experiments, we inoculated tumor cells into the tongue of BALB/c *nu/nu* mice and confirmed the formation of tumors with a diameter of 3 to 5 mm after 5 days and the development of metastases in neck lymph nodes after 35 days. We also identified the presence of disseminated tumor cells in the regional lymph nodes at least 10 days after tumor cell implantation by using GFP-expressing SAS-L human SCCHN cells (data not shown). Intratumoral injection of OBP-301 done 7 or 10 days after tumor inoculation significantly shrunk the tongue SAS-L tumor volumes, which in turn increased the body weight of mice by enabling oral ingestion (Fig. 3D). Moreover, HSC-3 cells were relatively resistant to OBP-301 *in vitro*; intratumoral injection of OBP-301 was, however, effective for recovering the body weight in mice bearing HSC-3 tongue tumors after a long-term observation (Supplementary Fig. S4). These results suggest that although the appearance of the effect may be slower, the *in vivo* antitumor activity could be

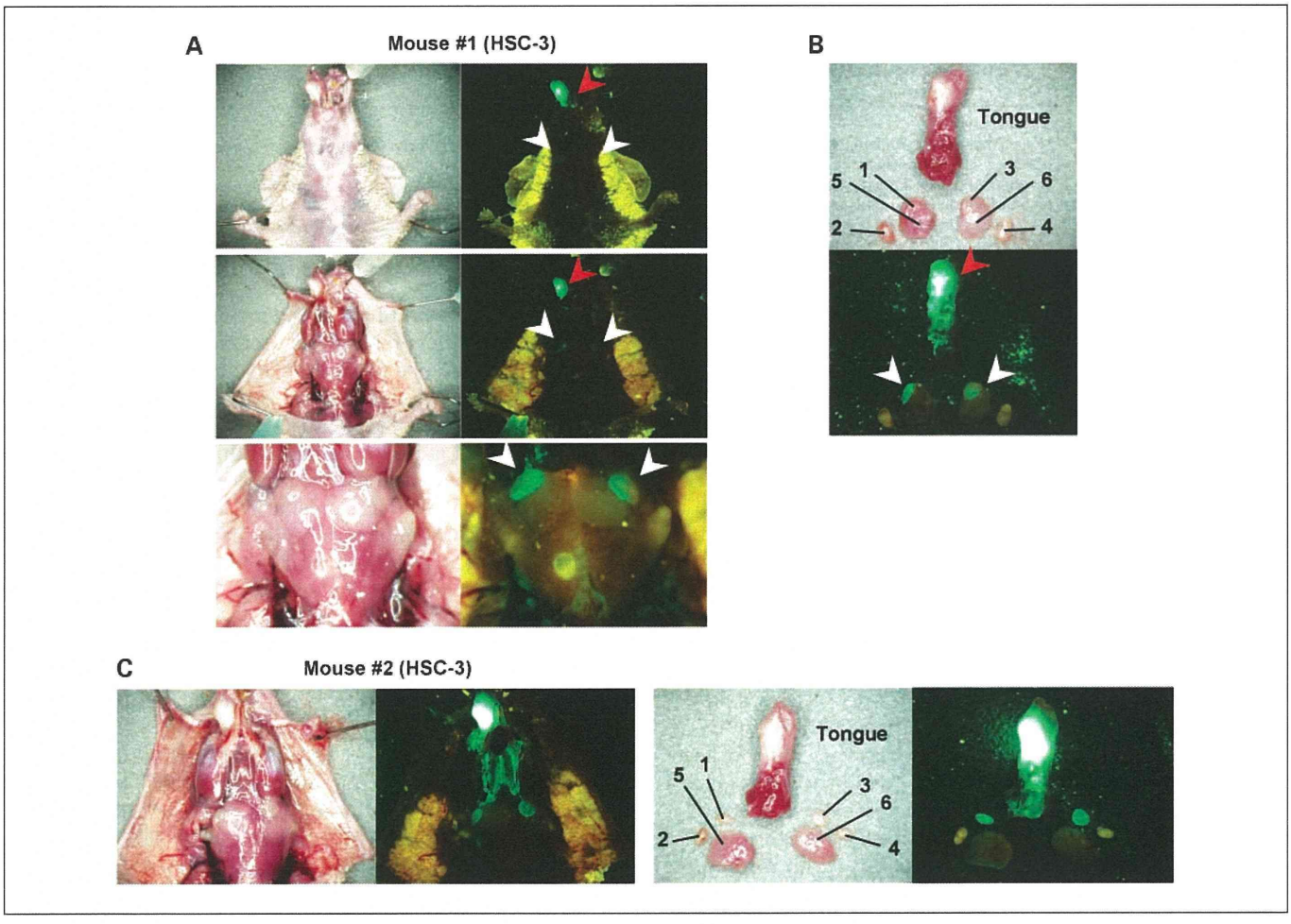

Fig. 5. Virus spread of OBP-401 via lymphatics to regional lymph nodes on HSC-3 tumor-bearing mice. *A,* selective visualization of lymph node metastasis in orthotopic xenografts of HSC-3 human SCCHN cells. Mice received intratumoral injection of OBP-401 at the concentration of 1×10^8 pfu after 24 d of tumor inoculation and were assessed for lymph node metastasis 5 d later under fluorescence stereomicroscope. *B,* HSC-3 primary tumor, salivary glands, and lymph nodes were excised 5 d after OBP-401 injection and then assessed for GFP fluorescence. 1 to 4, lymph nodes; 5 and 6, salivary glands. *C,* other HSC-3 tumor-bearing mice. Excised primary tumors, salivary glands, and lymph nodes were assessed for GFP fluorescence.

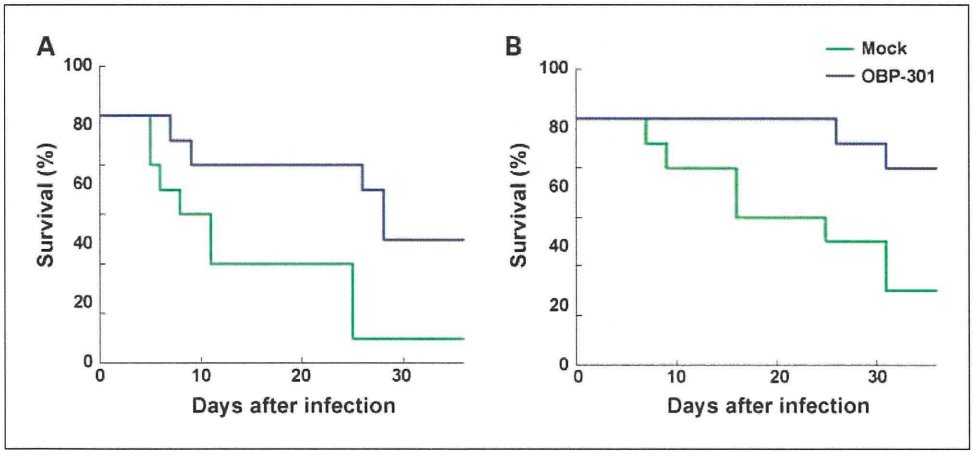

Fig. 6. Prolonged survival of SAS-L tumor-bearing mice treated with OBP-301. Mice bearing SAS-L xenografts were treated starting on day 7 (regimen 1; *A*) or day 10 (regimen 2; *B*) after tumor cell inoculation as described in Fig. 3A. Survival was monitored over time after virus injection and plotted as a Kaplan-Meier plot.

expected even in resistant SCCHN tumors. Because the body weight loss due to a feeding problem in this orthotopic SCCHN model resembles the disease progression in SCCHN patients, the finding that OBP-301 increased the body weight of mice suggests that OBP-301 virotherapy could potentially improve the quality of life in advanced SCCHN patients.

Amplified viruses can infect adjacent tumor cells as well as reach metastatic lymph nodes via the lymphatic circulation. We have previously shown that the telomerese-specific OBP-401–expressing GFP could be delivered into human tumor cells in regional lymph nodes and replicate with selective GFP fluorescence after injection into the primary tumor in an orthotopic rectal tumor model (11). In the orthotopic SCCHN model, OBP-401 spread into the neck lymph nodes after injection into the primary tongue tumor and selectively replicated in metastatic nodules (Figs. 4 and 5; Supplementary Fig. S5). The sensitivity and specificity of this imaging strategy for SAS-L tumors are 92.9% and 85.7%, respectively, which are sufficiently reliable to support the concept of this approach. These results suggest that surgeons may be able to excise primary tumors as well as metastatic lymph nodes precisely with appropriate margins by using this novel surgical navigation system with OBP-401. Moreover, the therapeutic profiles of OBP-401 and OBP-301 are considered similar, and a histopathologic analysis showed the destruction of micrometastases by virus in metastatic lymph nodes. This regional antitumor effect of oncolytic viruses could have a significant effect on the prolongation of the survival of mice bearing orthotopic tumors (Fig. 6).

Targeted therapies such as the anti–epidermal growth factor receptor monoclonal antibody cetuximab and other small-molecule epidermal growth factor receptor–tyrosine kinase inhibitors have been developed for SCCHN. Although a phase III trial showed a survival benefit with cetuximab and standard platinum-based therapy in SCCHN patients (23), some patients are exquisitely sensitive to these drugs and can develop particular and severe toxicities (24). A phase I study is currently under way in the United States to determine the feasibility and to characterize the pharmacokinetics of OBP-301 in patients with histologically proven nonresectable solid tumors (25). An interim analysis of the first 12 patients, including four SCCHN patients treated with escalating doses of OBP-301, indicates that OBP-301 virotherapy is well tolerated without any severe adverse events, suggesting that OBP-301 may be much more potent than other targeted therapies for human SCCHN in terms of specificity, efficacy, and toxicity.

In conclusion, our data clearly indicate that telomerase-specific oncolytic adenoviruses have a significant therapeutic potential against human SCCHN *in vitro* and *in vivo*. Moreover, these viruses can be used in an *ex vivo* diagnostic assay to predict the therapeutic potential of the virus in SCCHN patients. The combination of a diagnostic assay with a therapeutic entity is termed theranostics (26). Telomerase-specific oncolytic viruses can be used to treat the patients and to identify the patients who will likely benefit from virotherapy (Supplementary Fig. S6). In addition, telomerase-specific *in situ* imaging strategy has a potential of being widely available in humans as a navigation system in the surgical treatment of SCCHN. Thus, our oncolytic virus–based approach might be a novel "virotheranostics" for SCCHN. Phase II studies of telomerase-specific virotheranostics in advanced SCCHN patients are warranted.

Disclosure of Potential Conflicts of Interest

H. Onimatsu and Y. Urata are employed by Oncolys BioPharma, Inc. T. Fujiwara is a consultant to Oncolys Biopharma, Inc.

Acknowledgments

We thank Daiju Ichimaru and Hitoshi Kawamura for their helpful discussions and Tomoko Sueishi for her excellent technical support.

References

1. Parkin DM, Bray F, Ferlay J, Pisani P. Global cancer statistics, 2002. CA Cancer J Clin 2005;55:74–108.
2. Jemal A, Clegg LX, Ward E, et al. Annual report to the nation on the status of cancer, 1975–2001, with a special feature regarding survival. Cancer 2004;101:3–27.
3. Vokes EE, Weichselbaum RR, Lippman SM, Hong WK. Head and neck cancer. N Engl J Med 1993;328:184–94.
4. Vokes EE, Crawford J, Bogart J, Socinski MA, Clamon G, Green MR. Concurrent chemoradiotherapy for unresectable stage III non-small cell lung cancer. Clin Cancer Res 2005;11:5045–50s.
5. Milas L, Mason KA, Liao Z, Ang KK. Chemoradiotherapy: emerging treatment improvement strategies. Head Neck 2003;25:152–67.
6. Kirn D, Martuza RL, Zwiebel J. Replication-selective virotherapy for cancer: biological principles, risk management and future directions. Nat Med 2001;7:781–7.
7. Hawkins LK, Lemoine NR, Kirn D. Oncolytic

biotherapy: a novel therapeutic plafform. Lancet Oncol 2002;3:17–26.

8. Kawashima T, Kagawa S, Kobayashi N, et al. Telomerase-specific replication-selective virotherapy for human cancer. Clin Cancer Res 2004;10:285–92.

9. Taki M, Kagawa S, Nishizaki M, et al. Enhanced oncolysis by a tropism-modified telomerase-specific replication-selective adenoviral agent OBP-405 ('Telomelysin-RGD'). Oncogene 2005;24:3130–40.

10. Hashimoto Y, Watanabe Y, Shirakiya Y, et al. Establishment of biological and pharmacokinetic assays of telomerase-specific replication-selective adenovirus. Cancer Sci 2008;99:385–90.

11. Kishimoto H, Kojima T, Watanabe Y, et al. *In vivo* imaging of lymph node metastasis with telomerase-specific replication-selective adenovirus. Nat Med 2006;12:1213–9.

12. Kotwall C, Sako K, Razack MS, Rao U, Bakamjian V, Shedd DP. Metastatic patterns in squamous cell cancer of the head and neck. Am J Surg 1987;154: 439–42.

13. Myers JN, Holsinger FC, Jasser SA, Bekele BN, Fidler IJ. An orthotopic nude mouse model of oral tongue squamous cell carcinoma. Clin Cancer Res 2002;8:293–8.

14. Fujiwara T, Kagawa S, Kishimoto H, et al. Enhanced antitumor efficacy of telomerase-selective oncolytic adenoviral agent OBP-401 with docetaxel: preclinical evaluation of chemovirotherapy. Int J Cancer 2006; 119:432–40.

15. Riley T, Sontag E, Chen P, Levine A. Transcriptional control of human p53-regulated genes. Nat Rev Mol Cell Biol 2008;9:402–12.

16. Lefebvre JL. Current clinical outcomes demand new treatment options for SCCHN. Ann Oncol 2005;16 Suppl 6:vi7–12.

17. Endo Y, Sakai R, Ouchi M, et al. Virus-mediated oncolysis induces danger signal and stimulates cytotoxic T-lymphocyte activity via proteasome activator upregulation. Oncogene 2008;27:2375–81.

18. Ito H, Aoki H, Kühnel F, et al. Autophagic cell death of malignant glioma cells induced by a conditionally replicating adenovirus. J Natl Cancer Inst 2006;98: 625–36.

19. Sarker D, Workman P. Pharmacodynamic biomarkers for molecular cancer therapeutics. Adv Cancer Res 2007;96:213–68.

20. Fidler IJ. Rationale and methods for the use of nude mice to study the biology and therapy of human cancer metastasis. Cancer Metastasis Rev 1986;5:29–49.

21. Fidler IJ, Naito S, Pathak S. Orthotopic implantation is essential for the selection, growth and metastasis of human renal cell cancer in nude mice. Cancer Metastasis Rev 1990;9:149–65.

22. Killion JJ, Radinsky R, Fidler IJ. Orthotopic models are necessary to predict therapy of transplantable tumors in mice. Cancer Metastasis Rev 1998;17: 279–84.

23. Langer CJ. Targeted therapy in head and neck cancer: state of the art 2007 and review of clinical applications. Cancer 2008;112:2635–45.

24. Widakowich C, de Castro G, Jr., de Azambuja E, Dinh P, Awada A. Review: side effects of approved molecular targeted therapies in solid cancers. Oncologist 2007;12:1443–55.

25. Fujiwara T, Tanaka N, Nemunaitis J, et al. Phase I trial of intratumoral administration of OBP-301, a novel telomerase-specific oncolytic virus, in patients with advanced solid cancer: Evaluation of biodistribution and immune response. 2008 ASCO Annual Meeting Proceedings. J Clin Oncol 2008; 26:3572.

26. Del Vecchio S, Zannetti A, Fonti R, Pace L, Salvatore M. Nuclear imaging in cancer theranostics. Q J Nucl Med Mol Imaging 2007;51:152–63.

Invest New Drugs (2009) 27:241–245
DOI 10.1007/s10637-008-9169-5

PRECLINICAL STUDIES

Antiviral activity of cidofovir against telomerase-specific replication-selective oncolytic adenovirus, OBP-301 (Telomelysin)

Masaaki Ouchi · Hitoshi Kawamura · Yasuo Urata · Toshiyoshi Fujiwara

Received: 15 June 2008 / Accepted: 30 July 2008 / Published online: 27 August 2008

Summary We constructed a replication-competent oncolytic adenovirus, OBP-301 (Telomelysin), in which human telomerase reverse transcriptase (hTERT) promoter drives E1 genes. OBP-301 is currently being used in a phase-I clinical trial for various types of tumors. Under such conditions, anti-adenoviral agents should be available for safety use against OBP-301 since any adenoviral viremia could cause severe adverse effects. Cidofovir (CDV) is an acyclic nucleoside phosphonate that has a broad antiviral activity against DNA viruses. Here, we examined the antiviral effects of CDV against OBP-301. The *in vitro* cytopathic effects of OBP-301 were suppressed by CDV. Moreover, CDV decreased the adenoviral E1A gene copy number after OBP-301 infection. These results suggest that CDV is a potentially useful antiviral agent for OBP-301.

Keywords hTERT · Adenovirus · Cidofovir · Oncolytic virus · Clinical trial

Introduction

Oncolytic adenoviruses have been developed for treatment of human cancer. These viruses are designed to replicate and selectively kill cancer cells but to have minimum effect on normal cells [1]. Two major approaches to generate selective replication of viruses within tumor cells have been used [2, 3]. One is to delete genes that are critical for replication of the virus in normal cells but are dispensable for cancer cells such as ONYX-015 or Δ24 [4]. The other approach is the replacement of the promoter region that initiates viral replication genes to the promoter region of the genes active in cancer cells [2, 3]. Various genetic or epigenetic targets limited to cancer cells have been investigated and used for constructing oncolytic adenoviruses.

Human telomerase reverse transcriptase (hTERT) is an enzymatic subunit of human telomerase [5]. Telomerase is expressed in almost all cancer cells but not in all normal cells [6]. Therefore, telomerase is an attractive target for treatment of cancer. We constructed previously the attenuated adenovirus, OBP-301 (Telomelysin), in which adenoviral E1A and E1B genes are linked with internal ribosomal entry site under the control of the hTERT promoter. We reported that OBP-301 induced selective expression of E1A and E1B genes in many cancer cell lines and selectively replicated and lysed cancer cells but not normal cells [7–9]. OBP-301 is currently being tested in a phase-I clinical trial that includes various types of solid tumors. Although patients receiving this type of therapy become positive for anti-adenoviral neutralizing antibodies, those treated with OBP-301 could develop adenoviral viremia with potentially severe adverse effects. Thus, there is a need for anti-adenoviral agents for treatment of potential viremia in clinical trials of OBP-301.

One of the antiviral compounds is phosphonyl acyclic nucleotides, (S)-9-(3-hydroxy-2-phosphonometoxy propyl) cytosine dehydrate, also known as HPMPC (cidofovir, or CDV). CDV was developed for the treatment of viral infections and has a broad antiviral activity against DNA viruses, such as cytomegalovirus and adenoviruses (AdV). CDV exhibits potent inhibitory effects against several

M. Ouchi · H. Kawamura · Y. Urata
Oncolys BioPharma, Inc.,
Tokyo 106-0032, Japan

T. Fujiwara (✉)
Center for Gene and Cell Therapy, Okayama University Hospital,
Okayama 700-8558, Japan
e-mail: toshi_f@md.okayama-u.ac.jp

adenoviral serotypes in cell culture models [10]. Furthermore, CDV has been used clinically for AdV infections after bone marrow transplantation in immunodeficient patients [11]. Thus, we presumed that CDV could be a useful antiviral drug against OBP-301. In the present study, we examined the *in vitro* inhibitory effects of CDV against OBP-301 in human lung cancer cell lines.

Materials and methods

Cell culture, viruses, and chemicals

The human non-small lung cancer cell H1299 and lung cancer cell line A549 were purchased from American Type Culture Collection (ATCC). H1299 was cultured in RPMI 1640 medium supplemented with 10% FCS. A549 was cultured in DMEM F12 medium supplemented with 10% fetal calf serum (FCS). OBP-301 was constructed and characterized as described previously [7-9]. The human wild-type adenovirus type 5 (wt-Ad) was also used. VISTIDE™ (CDV injection) was purchased from Gilead Sciences (Foster City, CA).

Cell viability assay

Cells were seeded in 96-well plate at 1×10^3 cells per well and incubated at 37°C. After incubation, cells were infected with OBP-301 at a MOI of 1 (in H1299) and 5 (in A549) for 2 hours. The medium was aspirated and replaced with fresh medium containing 2% FCS and serially diluted CDV. Cell viability was determined by XTT assay 7 days after infection using Cell Proliferation Kit II (Roche Molecular Biochemicals) according to the protocol recommended by the manufacturer. Protection was determined by the following formula: Protection (%)={OD (AdV(+):CDV (+)) − OD (AdV (+):CDV(−))}/{OD (AdV(−):CDV(+)) −OD (AdV (+):CDV(−))}×100. CC_{50} (50% cytotoxic concentration) was defined as CDV concentration that inhibited relative cell viability to 0.5 without OBP-301 infection. EC_{50} (50% effective concentration) was defined as CDV concentration that archived 50% protection.

Quantitative real-time PCR analysis

Cells were seeded in six-well plate at 2×10^5 cells per well. After overnight incubation at 37°C, the medium was aspirated, and cells were infected with OBP-301 or wt-Ad at a MOI of 10 for 2 hours at 37°C with gentle shaking every 15 minutes. After incubation, the cells were washed with PBS and placed in a medium containing serially diluted CDV (100, 20, 4, 0.8, 0.16 and 0 μM). The cells were harvested 24 hours later with Trypsin/EDTA and total DNA was extracted using QIAamp™ DNA Mini Kit (Qiagen, Hilden, Germany). Viral E1A copy number was measured using LightCycler instruments and LightCycler Faststart DNAMaster SYBR Green I (Roche, Mannheim, Germany). EC_{50} (E1A) was defined as the CDV concentration that inhibits the E1A ratio (with CDV/no CDV) to 0.5. Primers for E1A gene were: forward: 5'- CCTGTGTCTA GAGAATGCAA -3', reverse: 5'- ACAGCTCAAGTC CAAAGGTT - 3'. PCR amplification began with a 600-s of denaturation step at 95°C and then 40 cycles of denaturation at 95°C for 10 s, annealing at 60°C for 15 s, and extension at 72°C for 8 s.

Statistical analysis

The Student's *t*-test was used to compare differences. Statistical significance was defined when p was <0.05.

Results

In vitro cytopathic effect of OBP-301 on lung cancer cell lines

We reported previously that OBP-301 exhibited oncolytic activity against many types of human cancer cells [7–9]. To confirm this, we tested its cytopathic effects in cancer cell line *in vitro*. Human lung cancer cell lines, A549 and H1299, were infected with OBP-301 at various MOIs and numbers of living cells were measured by XTT assay (Fig. 1). At 5 days after infection, the majority of H1299 cells were killed by OBP-301 at MOI of 1 and 10, and approximately 70% of A549 cells were killed by OBP-301 at MOI of 50. These results confirmed that OBP-301 induced cell death in A549 and H1299 cells.

Inhibitory effects of CDV on the cytopathic effect of OBP-301

Next, we tested whether the cytopathic effect by OBP-301 on these cancer cells could be inhibited by CDV treatment. A549 and H1299 cells were infected with OBP-301 then treated with CDV at various concentrations. Cell viability was also determined by XTT assay. In the presence of the drug and virus, relative cell viability significantly increased in the presence of CDV at > 30 μM in A549 cells and > 40 μM in H1299 cells ($p<0.01$) (Fig. 2). Furthermore, inhibition of cell growth of each cell line was observed in the presence of CDV at > 100 μM. The calculated EC_{50} values of CDV were 20.4 μM for H1299 and 35.9 μM for A549 cells, while the calculated CC_{50} values were 146.4 μM for H1299 cells and 106.9 μM for A549 cells. Similar results were obtained by using ONYX-015 (see

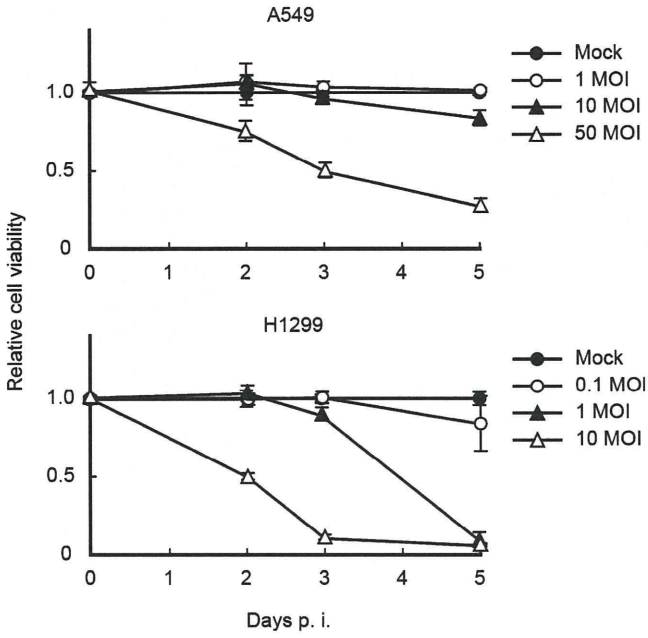

Fig. 1 Cytopathic effects of OBP-301 on H1299 and A549 lung cancer cell lines *in vitro*. Each cell was infected with OBP-301 at the indicated MOI and cell viability was evaluated by XTT assay (no virus=1.0). Data are mean±SD values

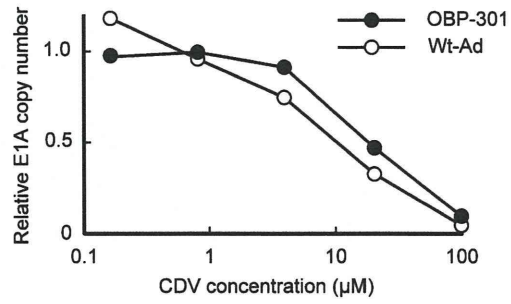

Fig. 3 Inhibition of OBP-301 replication in H1299 cells by CDV. Cells were infected with OBP-301 or wild-type AdV at MOI of 10, followed by the addition of CDV at the indicated concentrations. Cells were collected after 24 hours infection, total DNA was extracted, and viral E1A copy number was determined by quantitative real-time PCR analysis (with virus/no CDV=1.0)

Introduction) and OBP-401, a modified OBP-301 that contains the GFP gene [12] (data not shown).

Inhibitory effects of CDV on viral replication of OBP-301

Finally, we examined whether CDV inhibits the replication of OBP-301 *in vitro*. We previously used two methods to quantify viral replication, biological plaque forming assay using 293 cells [7] and real-time PCR assay targeting adenoviral E1A sequence [8, 9], and found that both assays could detect viral replication similarly. H1299 cells were infected with OBP-301 or wt-Ad, followed by treatment with CDV. Wt-Ad was used for positive control in this assay since it had been reported that CDV had antiviral activity against wt-Ad. To measure the viral DNA, we quantified E1A copy number of cells infected with OBP-301 or wt-Ad by real-time PCR assay. CDV reduced the relative E1A copy number in both wt-Ad and OBP-301-infected cells and the effect was concentration-dependent, indicating that CDV inhibited viral replication of OBP-301 and wt-Ad in H1299 cells (Fig. 3). The calculated EC_{50} (E1A) value for OBP-301 was 19.55 μM.

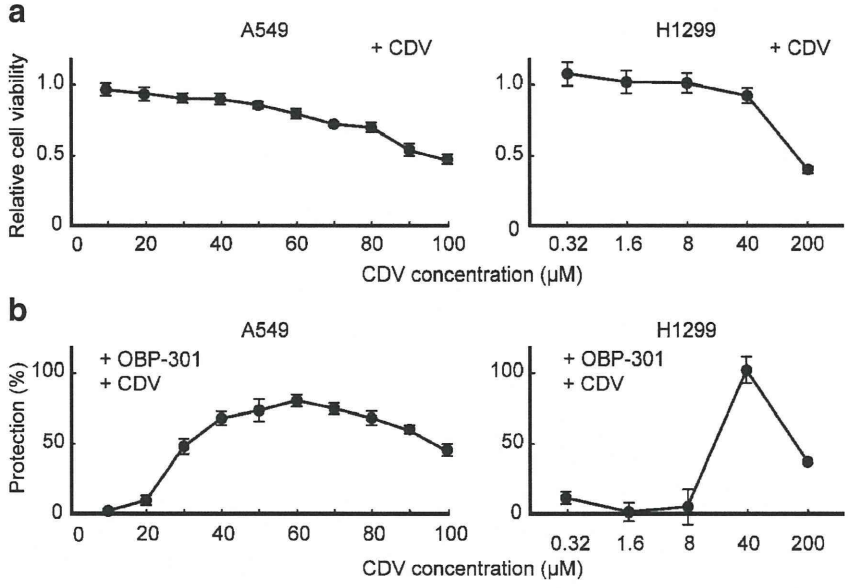

Fig. 2 Inhibition of cytopathic effects of OBP-301 by CDV in human lung cancer cell lines. (**a**) Cells were treated with CDV at the indicated concentrations and incubated for 7 days. The relative cell viability was evaluated by XTT assay. Data are mean±SD values. (**b**) Cells were infected with OBP-301 (1 MOI in H1299 and 5 MOI in A549, PFU/cell), followed by the addition of CDV at the indicated concentrations. Protection was calculated as described in "Material and methods". Data are mean±SD values

Discussion

OBP-301 has been developed as an oncolytic viral agent for the treatment of human cancer and is currently used in a phase-I clinical trial. Although replication of OBP-301 is limited in normal cells evaluated *in vitro* and *in vivo* mouse model, the effect of OBP-301 in human is still unknown. In the phase-II clinical trial of ONYX-015, an E1B-55 kDa-deleted adenovirus mutant, adenoviral viremia occurred even in the presence of neutralizing antibodies and antiviral cytokines [13]. Several antiviral drugs are used for other DNA viruses, e.g. aciclovir, a synthetic acyclic purine-nucleoside analogue, for Herpes simplex virus (HSV) [14], and ganciclovir (GCV) for Cytomegalovirus infections [15]. For AdV infections, it has been reported that CDV exhibits potent inhibitory effects against several adenoviral serotypes in cell culture models [10, 16]. We considered that CDV can be used as antiviral drug for OBP-301.

The purpose of using CDV clinically is to avoid toxic effects of OBP-301 in normal tissues, when viral replication becomes uncontrollable. However, it is difficult to examine the inhibitory effect of CDV on cytopathic effect of OBP-301 in normal cells, because OBP-301 replicates and lyses only in cancer cells [7–9]. Therefore, we used human cancer cell lines to assess the potential antiviral activity of CDV. We showed that the cytopathic effects of OBP-301 were efficiently suppressed by CDV treatment at concentrations that did not affect cell growth (Fig. 2). Despite the high susceptibility of H1299 cells to OBP-301 infection (Fig. 1), CDV inhibited the cytopathic effects of OBP-301, suggesting that CDV has potent antiviral activity against OBP-301. The 50% effective concentration of CDV in A549 cells was in agreement with the published data using human wt-Ad [17], indicating that the inhibitory activity against the cytopathic effect of OBP-301 was equivalent to that of wt-Ad.

The mechanism of the antiviral effect of CDV is that of inhibition of viral replication by targeting the viral DNA polymerase [18]. The anti-adenoviral effect of CDV is quantified by evaluating the viral progeny in adenovirus-infected cells using quantitative PCR analysis [16]. We demonstrated that the replication of OBP-301 was inhibited by CDV in a concentration-dependent manner (Fig. 3). In addition, the 50% effective concentration on viral DNA copy number was almost the same as the 50% effective concentration on cell death by OBP-301 infection, suggesting that CDV inhibited the cytopathic effect of OBP-301 by inhibiting the replication of OBP-301. Recently, antiviral effect of CDV against wt-Ad in immunosuppressed Syrian hamster model was reported [19]. The 50% inhibitory concentration of CDV on viral DNA copy number in OBP-301 was slightly higher than that of wt-Ad (Fig. 3). Differences at E1A region between OBP-301 and wt-Ad may affect of CDV activity on viral replication. It has been reported that CDV-resistant human Ad mutants were isolated by continuous passage *in vitro* condition [20]. Quality assurance and quality control of the master virus bank have been intensively performed for OBP-301 used in the current clinical trials; emergence of CDV-resistant OBP-301 variant, however, should be considered and long-term susceptibility of CDV against OBP-301 will be studied in the future clinical trials.

In conclusion, our *in vitro* data indicate that CDV can effectively inhibit the oncolytic activity of OBP-301 by inhibiting the replication of OBP-301. CDV may be a potential antiviral agent for OBP-301 in clinical trial.

References

1. Kirn D, Martuza RL, Zwiebel J (2001) Replication-selective virotherapy for cancer: biological principles, risk management and future directions. Nat Med 7:781–787. doi:10.1038/89901
2. Kirn D (2000) Replication-selective oncolytic adenoviruses: virotherapy aimed at genetic targets in cancer. Oncogene 19:6660–6669. doi:10.1038/sj.onc.1204094
3. Chu RL, Post DE, Khuri FR, Van Meir EG (2004) Use of replicating oncolytic adenoviruses in combination therapy for cancer. Clin Cancer Res 10:5299–5312. doi:10.1158/1078-0432.CCR-0349-03
4. Davis JJ, Fang B (2005) Oncolytic virotherapy for cancer treatment: challenges and solutions. J Gene Med 7:1380–1389. doi:10.1002/jgm.800
5. Nakamura TM, Morfin GB, Chapman KB, Weinrich SL, Andrews WH, Lingner J et al (1997) Telomerase catalytic subunit homologs from fission yeast and human. Science 277:955–959. doi:10.1126/science.277.5328.955
6. Kim NW, Piatyszek MA, Prowse KR, Harley CB, West MD, Ho PL et al (1994) Specific association of human telomerase activity with immortal cells and cancer. Science 266:2011–2015. doi:10.1126/science.7605428
7. Kawashima T, Kagawa S, Kobayashi N, Shirakiya Y, Umeoka T, Teraishi F et al (2004) Telomerase-specific replication-selective virotherapy for human cancer. Clin Cancer Res 10:285–292. doi:10.1158/1078-0432.CCR-1075-3
8. Taki M, Kagawa S, Nishizaki M, Mizuguchi H, Hayakawa T, Kyo S et al (2005) Enhanced oncolysis by a tropism-modified telomerase-specific replication-selective adenoviral agent OBP-405 (Telomelysin-RGD). Oncogene 24:3130–3140. doi:10.1038/sj.onc.1208460
9. Hashimoto Y, Watanabe Y, Shirakiya Y, Uno F, Kagawa S, Kawamura H et al (2008) Establishment of biological and pharmacokinetic assays of telomerase-specific replication-selective adenovirus. Cancer Sci 99:385–390. doi:10.1111/j.1349-7006.2007.00665.x
10. Gordon YJ, Romanowski E, Araullo-Cruz T, Seaberg L, Erzurum S, Tolman R et al (1991) Inhibitory effect of (S)-HPMPC, (S)-HPMPA, and 2'¢-nor-cyclic GMP on clinical ocular adenoviral isolates is serotype-dependent in vitro. Antivir Res 16:11–16. doi:10.1016/0166-3542(91)90054-U
11. De Clercq E (2003) Clinical potential of the acyclic nucleoside phosphonates cidofovir, adefovir, and tenofovir in treatment of DNA virus and retrovirus infections. Clin Microbiol Rev 16:569–596. doi:10.1128/CMR.16.4.569-596.2003

12. Kishimoto H, Kojima T, Watanabe Y, Kagawa S, Fujiwara T, Uno F et al (2006) *In vivo* imaging of lymph node metastasis with telomerase-specific replication-selective adenovirus. Nat Med 12:1213–1219. doi:10.1038/nm1404
13. Reid T, Galanis E, Abbruzzese J, Sze D, Wein LM, Andrews J et al (2002) Hepatic arterial infusion of a replication-selective oncolytic adenovirus (dl1520): phase II viral, immunologic, and clinical endpoints. Cancer Res 62:6070–6079
14. Whitley RJ, Roizman B (2001) Herpes simplex virus infection. Lancet 357:1513–1518. doi:10.1016/S0140-6736(00)04638-9
15. Biron KK (2006) Antiviral drugs for cytomegalovirus diseases. Antivir Res 71:154–163. doi:10.1016/j.antiviral.2006.05.002
16. Naesens L, Lenaerts L, Andrei G, Snoeck R, Van Beers D, Holy A et al (2005) Antiadenovirus activities of several classes of nucleoside and nucleotide analogues. Antimicrob Agents Chemother 49:1010–1016. doi:10.1128/AAC.49.3.1010-1016.2005
17. Morfin F, Dupuis-Girod S, Mundweiler S, Falcon D, Carrington D, Sedlacek P et al (2005) *In vitro* susceptibility of adenovirus to antiviral drugs is species-dependent. Antivir Ther 10:225–229
18. Kinchington PR, Araullo-Cruz T, Vergnes JP, Yates K, Gordon YJ (2002) Sequence changes in the human adenovirus type 5 DNA polymerase associated with resistance to the broad spectrum antiviral cidofovir. Antivir Res 56:73–84. doi:10.1016/S0166-3542(02)00098-0
19. Toth K, Spencer JF, Dhar D, Sagartz JE, Buller RM, Painter GR et al (2008) Hexadecyloxypropyl-cidofovir, CMX001, prevents adenovirus-induced mortality in a permissive, immunosuppressed animal model. Proc Natl Acad Sci U S A 105:7293–7297. doi:10.1073/pnas.0800200105
20. Gordon YJ, Araullo-Cruz TP, Johnson YF, Romanowski EG, Kinchington PR (1996) Isolation of human adenovirus type 5 variants resistant to the antiviral cidofovir. Invest Ophthalmol Vis Sci 37:2774–2778

Preclinical evaluation of synergistic effect of telomerase-specific oncolytic virotherapy and gemcitabine for human lung cancer

Dong Liu,[1,3] Toru Kojima,[1,2] Masaaki Ouchi,[4] Shinji Kuroda,[1,2] Yuichi Watanabe,[2,4] Yuuri Hashimoto,[2,4] Hideki Onimatsu,[4] Yasuo Urata,[4] and Toshiyoshi Fujiwara[1,2]

[1]Center for Gene and Cell Therapy, Okayama University Hospital; [2]Division of Surgical Oncology, Department of Surgery, Okayama University Graduate School of Medicine, Dentistry and Pharmaceutical Sciences, Okayama, Japan; [3]Research Center of Lung Cancer, Shanghai Pulmonary Hospital, The Tongji University, Shanghai, China; and [4]Oncolys BioPharma, Inc., Tokyo, Japan

Abstract

A phase I dose-escalation study of telomerase-specific oncolytic adenovirus, OBP-301 (Telomelysin), is now under way in the United States to assess feasibility and to characterize its pharmacokinetics in patients with advanced solid tumors. The present preclinical study investigates whether OBP-301 and a chemotherapeutic agent that is commonly used for lung cancer treatment, gemcitabine, are able to enhance antitumor effects *in vitro* and *in vivo*. The antitumor effects of OBP-301 infection and gemcitabine were evaluated by 2,3-bis[2-methoxy-4-nitro-5-sulfophenyl]-2H-tetrazolium-5-carboxanilide inner salt assay. *In vivo* antitumor effects of intratumoral injection of OBP-301 in combination with systemic administration of gemcitabine were assessed on *nu/nu* mice s.c. xenografted with human lung tumors. OBP-301 infection combined with gemcitabine resulted in very potent synergistic cytotoxicity in human lung cancer cells. The three human lung cancer cell lines treated with OBP-301 for 24 hours tended to accumulate in S phase compared with controls. The proportion of cells in S phase increased from 43.85% to 56.41% in H460 cells, from 46.72% to 67.09% in H322 cells, and from 38.22% to 57.67% in H358 cells. Intratumoral injection of OBP-301 combined with systemic administration of gemcitabine showed therapeutic synergism in human lung tumor xenografts. Our data suggest that the combination of OBP-301 and gemcitabine enhances the antitumor effects against human lung cancer. We also found that the synergistic mechanism may be due to OBP-301–mediated cell cycle accumulation in S phase. These results have important implications for the treatment of human lung cancer. [Mol Cancer Ther 2009;8(4):980–7]

Introduction

Lung cancer is the most common cause of cancer-related mortality. In current clinical practice, chemotherapy is used in combination with radiotherapy as an adjuvant or neoadjuvant therapy. Moreover, combination chemotherapy is regarded as the standard care in the treatment of unresectable locally advanced (stage IIIB), metastatic (stage IV), or recurrent disease. Although there have been major improvements over recent decades in surgical techniques and the role of chemotherapy-radiotherapy in the treatment of non–small cell lung cancer, the long-term outlook for such patients has not changed significantly. The median survival for patients with advanced-stage non–small cell lung cancer treated with platinum-based chemotherapy is a disappointing 8 to 10 months (1). Clearly, new therapies are needed that are capable of treating such advanced cancers in addition to preventing their formation.

One type of cancer therapy that has been extensively investigated is virotherapy, which uses oncolytic viruses engineered to selectively replicate within tumor cells, killing them. We previously developed an adenovirus vector that drives the *E1A* and *E1B* genes under the hTERT promoter, designated OBP-301 (Telomelysin), and showed its selective replication, as well as its profound cytotoxic activity, in a variety of human cancer cells (2–5). Although the development of OBP-301 as a monotherapy is currently under way clinically based on the promising preclinical results, multimodal strategies to enhance antitumor efficacy *in vivo* are essential for successful clinical outcome. In fact, most clinical trials for oncolytic viruses have been conducted in combination with chemotherapy or radiotherapy (6).

Gemcitabine (2,2-difluorodeoxycytidine) is a third-generation agent that has been developed in the past decades. Gemcitabine is a deoxycytidine analogue that has shown efficacy as a treatment for many solid tumors and is now extensively used in the treatment of patients with various tumor types (7, 8), but inherent and acquired resistance has resulted in low response rates. In the present study, we hypothesized that combination of oncolytic adenoviral agents (with novel mechanisms of action) with

Received 9/19/08; revised 12/15/08; accepted 1/20/09.

Grant support: Ministry of Education, Science, and Culture, Japan (T. Fujiwara); Ministry of Health and Welfare, Japan (T. Fujiwara); and Japan China Medical Association (D. Liu).

The costs of publication of this article were defrayed in part by the payment of page charges. This article must therefore be hereby marked *advertisement* in accordance with 18 U.S.C. Section 1734 solely to indicate this fact.

Requests for reprints: Toshiyoshi Fujiwara, Center for Gene and Cell Therapy, Okayama University Hospital, 2-5-1 Shikata-cho, Okayama 700-8558, Japan. Phone: 81-86-235-7997; Fax: 81-86-235-7884. E-mail: toshi_f@md.okayama-u.ac.jp

doi:10.1158/1535-7163.MCT-08-0901

chemotherapeutic agents could improve the antitumor effects and minimize the toxic side effects of the latter by reducing the concentrations of anticancer drugs. To test our hypothesis, we examined the therapeutic effects of OBP-301 combined with gemcitabine both *in vitro* and *in vivo*. The results showed that combination therapy with OBP-301 and gemcitabine produced therapeutic benefits over either individual modality.

Materials and Methods

Cell Lines and Cell Cultures

The human large cell lung cancer cell line H460, the bronchioloalveolar carcinoma cell line H322, and the bronchioloalveolar carcinoma cell line H358 were propagated in monolayer culture in RPMI 1640 supplemented with 10% FCS.

Chemotherapeutic Agents and Viruses

Gemcitabine (Gemzar) was obtained from Eli Lilly Co. Stock solution was prepared in 0.9% NaCl and the agent was further diluted in growth medium immediately before use. OBP-301 is a telomerase-specific replication-competent adenovirus variant, in which the hTERT promoter element drives the expression of *E1A* and *E1B* linked with internal ribosomal entry site. The virus was purified by ultracentrifugation in cesium chloride step gradients and titer was determined by plaque assay in 293 cells, as described previously (2–5).

Cell Viability Assay

2,3-Bis[2-methoxy-4-nitro-5-sulfophenyl]-2H-tetrazolium-5-carboxanilide inner salt (XTT) assay was done to assess the viability of tumor cells. H460, H322, and H358 cells at 1,000 per well were seeded onto 96-well plates at 18 to 20 h before viral infection. Cells were then infected with OBP-301 at low to high concentrations and were treated with fresh medium containing gemcitabine at various concentrations at 24 h after OBP-301 infection. Cell viability was determined at 4 d after treatment with OBP-301 and gemcitabine by using a Cell Proliferation Kit II (Roche Molecular Biochemicals) according to the protocol provided by the manufacturer.

In vitro Replication Assay

H460, H322, and H358 cells were seeded in six-well plates at 10^5 per well at 12 h before infection. Cells were infected with OBP-301 at a multiplicity of infection (MOI) of 10, 25, and 20 plaque-forming units (pfu)/cell, respectively, and fresh medium containing gemcitabine at 70 nmol/L for H460 cells, 100 nmol/L for H322 cells, and 3 nmol/L for H358 cells was then added at 24 h after infection. Cells were incubated at 37°C, trypsinized, and harvested for intracellular replication analysis at 2, 24, 48, 72, 96, and 108 h after OBP-301 infection. DNA purification was done using QIAmp DNA Mini kit (Qiagen, Inc.). The E1A DNA copy number was determined by quantitative real-time PCR using a LightCycler instrument and LightCycler-DNA Master SYBR Green I (Roche Diagnostics).

Assessment of E1A Expression by Western Blotting

H460, H322, and H358 cells infected with OBP-301 at an MOI of 10, 25, and 20, respectively, were collected at 5 d after infection, lysed in lysis buffer [10 mmol/L Tris-HCl (pH 7.5), 400 mmol/L NaCl, 1 mmol/L DTT, 5 mmol/L NaF, 1 mmol/L EDTA, 0.5% Na_3VO_4, 10% glycerol, 0.5% NP40, 0.1 mmol/L phenylmethylsulfonyl fluoride, 1 mg/mL leupeptin, 1 mg/mL aprotinin] for 30 min on ice, and centrifuged at 15,000 rpm for 30 min. Protein concentration was measured by means of the Bradford assay. Equal amounts of protein-containing sample buffer [62.5 mmol/L Tris-HCl (pH 6.8), 2% SDS, 10% glycerol, 5% β-mercaptoethanol] were boiled for 5 min and electrophoresed under reducing conditions on 12% (w/v) polyacrylamide gels. Proteins were electrophoretically transferred to Hybond polyvinylidene difluoride transfer membranes (Amersham) and incubated with primary antibody against E1A (BD Pharmingen) or rabbit anti-human β-actin monoclonal antibody (Sigma-Aldrich) followed by peroxidase-linked secondary antibody. An enhanced chemiluminescence Western system (Amersham) was used to detect secondary probes.

Cell Cycle Analysis

H460, H322, and H358 cells were infected with OBP-301 at 40, 100, and 80 MOI, respectively, for 24 h. The cells were then harvested and suspended in 1.5 mL PBS before fixing with ice-cold 70% ethanol for 30 min. Fixed samples were centrifuged for 5 min, and cell pellets were resuspended in 700 μL PBS containing RNase (0.25 mg/mL) followed by incubation for 30 min at 37°C. The volume was increased to 1 mL with PBS containing 1% bovine serum albumin and propidium iodide (50 μg/mL) and the suspensions were incubated at 4°C for 30 min. Stained cells were analyzed by FACScan (Becton Dickinson) and by WinMDI v2.8 software (Scripps Institute).

Assessment of Cell Cycle Regulator Protein Expression by Western Blotting

H460, H322, and H358 cells were infected with OBP-301 at 40, 100, and 80 MOI, respectively, before harvesting 24 h later. Collected cells were analyzed for expression of E2F1, p53, and E1A and phosphorylation of Akt. Primary antibodies were purchased from Santa Cruz Biotechnology (E2F1), Calbiochem Co. (p53), and Sigma Co. (β-actin). Protein expression was quantified by densitometric scanning using NIH Image software.

In vivo Human Tumor Model

H358 cells (5×10^6 per mouse) were injected s.c. into the backs of 5- to 6-wk-old female BALB/c *nu/nu* mice and were permitted to grow to 5 to 10 mm in diameter. At that time, mice were randomly assigned into four groups: mock, OBP-301, gemcitabine, and OBP-301 plus gemcitabine. Next, 50 μL of solution containing OBP-301 at a dose of 1×10^7 pfu/body or PBS were injected into the tumors. Simultaneously, each mouse in the combination group and gemcitabine group received an i.p. injection of 100 μL gemcitabine at a dose of 70 mg/kg every 3 d for three cycles starting at day 0. The perpendicular

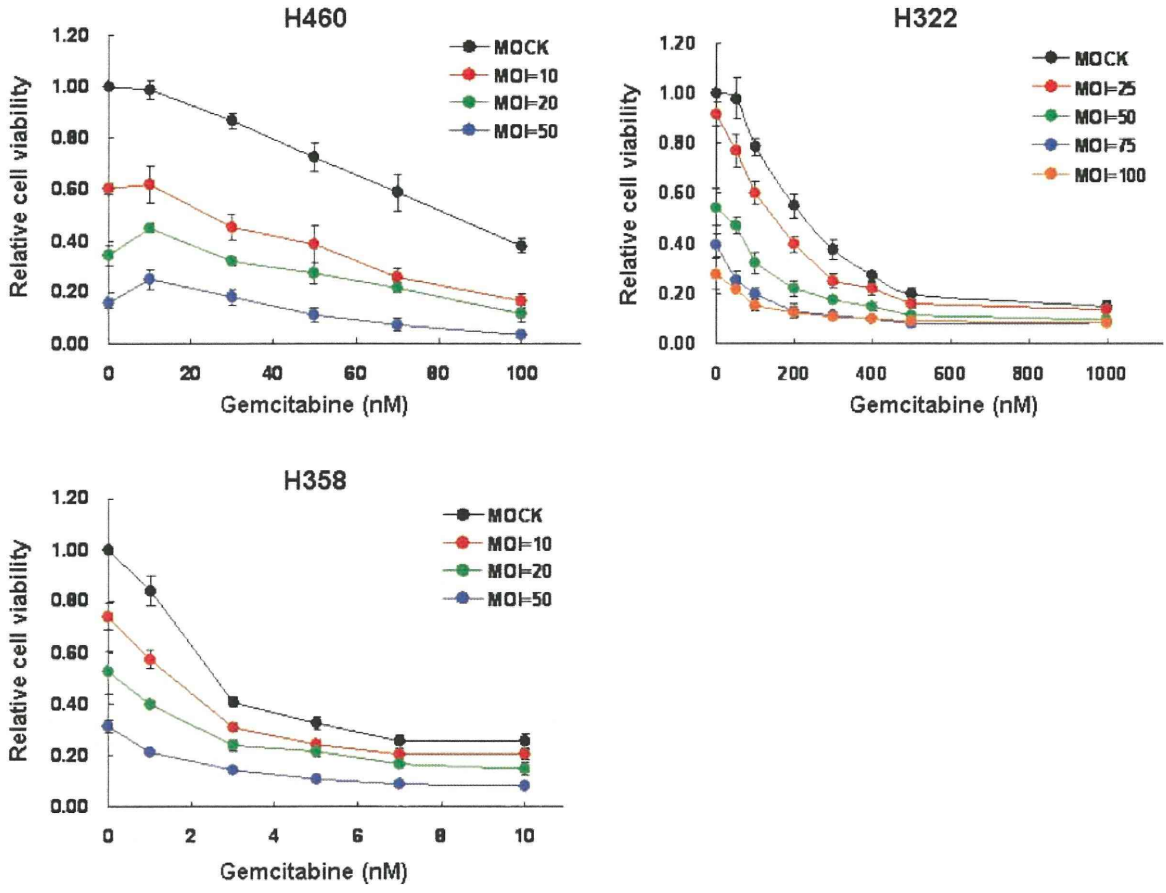

Figure 1. Combination efficiency of OBP-301 and gemcitabine on human lung cancer cell lines. H460, H322, and H358 cells were infected with OBP-301 at the indicated MOIs and then exposed to gemcitabine at the indicated concentrations at 24 h after infection. Cell viability was assessed by XTT assay at 5 d after OBP-301 infection. *Bars,* SD.

diameter of each tumor was measured every 3 d, and tumor volume was calculated using the following formula: tumor volume (mm^3) = $a \times b^2 \times 0.5$, where a is the longest diameter, b is the shortest diameter, and 0.5 is a constant used to calculate the volume of an ellipsoid. The experimental protocol was approved by the Ethics Review Committee for Animal Experimentation of Okayama University.

Statistical Analysis

Determinations of significant differences in mean tumor size among groups were assessed by calculating the value of Student's t using the original data analysis.

Results

Antitumor Efficacy of OBP-301 Combined with Gemcitabine in Human Lung Cancer Cell Lines *In vitro*

Before we tested the combination efficacy, sensitivity to gemcitabine and OBP-301 was evaluated in a variety of human lung cancer cell lines by the XTT method, and we selected three cell lines, H460, H322, and H358, for further experiments. From the XTT experiments with gemcitabine alone or OBP-301 alone (Supplementary Fig. S1),[5] the optimal concentrations of gemcitabine and OBP-301 were determined for each cell line. To examine the potential interaction between gemcitabine and OBP-301 *in vitro*, cell viability with six to eight different doses of OBP-301 and four to five doses of gemcitabine was then assessed by XTT assay at 5 days after treatment. Representative dose-response curves are shown in Fig. 1. All cell lines treated with OBP-301 and gemcitabine showed reduced viability when compared with cells treated with single agents.

We then used software to analyze the combination efficiency in these three cell lines (Table 1). In H358 cells, OBP-301 and gemcitabine were apparently synergistic at most doses, whereas the effect of the combination was mostly additive in H322 cells. In H460 cells, the effect was additive when the concentration of gemcitabine was 50 nmol/L; with the increasing of the concentration, however, a clear synergistic effect was seen. When the concentration was 100 nmol/L, synergism was apparent. These

[5] Supplementary data for this article are available at Molecular Cancer Therapeutics Online (http://mct.aacrjournals.org/).

Table 1. Combination index value analysis by CalcuSyn software (version 2) of combination efficiency in human lung cancer cells

Cells	Gemcitabine (nmol/L)	OBP-301 (MOI)	Combination index	Synergy
H460	10	10	1.261	––
		20	1.405	––
		50	1.688	––
	30	10	0.996	±
		20	1.106	–
		50	1.349	––
	50	10	1.037	±
		20	1.104	–
		50	0.998	±
	70	10	0.87	+
		20	1.037	±
		50	0.793	++
	100	10	0.793	++
		20	0.785	++
		50	0.531	+++
H358	1	10	0.952	±
		20	0.812	++
		50	0.772	++
	3	10	0.713	++
		20	0.674	+++
		50	0.641	+++
	5	10	0.792	++
		20	0.828	++
		50	0.613	+++
	7	10	0.88	+
		20	0.812	++
		50	0.596	+++
	10	10	1.178	–
		20	0.948	±
		50	0.693	+++
H322	50	25	1.028	±
		50	0.941	±
		75	0.874	++
		100	1.033	±
	100	25	0.953	±
		50	0.842	++
		75	0.848	++
		100	0.938	±
	200	25	0.944	±
		50	0.856	+
		75	0.82	++
		100	0.979	±
	300	25	0.912	±
		50	1.024	±
		75	0.887	+
		100	0.887	+
	400	25	1.005	±
		50	0.975	±
		75	1.093	±
		100	0.938	±
	500	25	0.977	±
		50	0.97	±
		75	0.946	±
		100	1.154	–

NOTE: Range of combination index symbol descriptions: 0.3 to 0.7, +++, synergism; 0.7 to 0.85, ++, moderate synergism; 0.85 to 0.90, +, slight synergism; 0.90 to 1.10, ±, additive; 1.10 to 1.20, –, slight antagonism; 1.20 to 1.45, ––, moderate antagonism.

results suggest that combination treatment with OBP-301 plus gemcitabine was effective in all cell lines tested.

We also assessed the morphologic changes in cells treated with either the combination modality or single agents. Phase-contrast images at 96 hours after OBP-301 infection showed the growth of cells to subconfluence without morphologic changes in the presence of gemcitabine, whereas a rapid loss of viability due to massive cell death, as evidenced by ballooning and floating cells, was evident when gemcitabine was combined with OBP-301 infection (Supplementary Fig. S2).[5]

Effects of Gemcitabine on Replication of OBP-301 in Human Lung Cancer Cells *In vitro*

We used quantitative real-time PCR and Western blotting to assess the effects of gemcitabine on replication of OBP-301 in the three lung cancer cell lines. H460, H322, and H358 cells were infected with OBP-301 at an MOI of 10, 25, and 20, respectively, and were then treated with 70, 100, and 3 nmol/L of gemcitabine at 24 hours after infection. Cells were harvested at the indicated time points after OBP-301 infection, and extracted DNA was subjected to assay. As shown in Fig. 2A, the increase in intracellular viral copy number of OBP-301 by 4 to 5 orders of magnitude was consistent with or without gemcitabine in both treatment regimens. A plateau was reached at ~48 hours after infection. Western blot analysis also showed that E1A expression following OBP-301 infection was not hindered by gemcitabine in three lung cancer cell lines (Fig. 2B). These results suggest that gemcitabine does not interfere with OBP-301 replication.

Cell Cycle Analysis following OBP-301 Infection in Human Lung Cancer Cells

To further explore the "greater than additive response" observed when cells were infected with OBP-301 followed by gemcitabine treatment, we carried out cell cycle analysis of these cells after OBP-301 infection by flow cytometric analysis of propidium iodide–stained cells, a measure of DNA content. As shown in Fig. 3A, the cell cycle distribution apparently changed compared with mock-infected cells at 24 hours after OBP-301 infection in all cell lines tested, although there was no increase in the sub-G_0-G_1 population indicating apoptotic cell death. The number of cells in S phase increased from 43.85% to 56.41% in H460 cells, from 46.72% to 67.09% in H322 cells, and from 38.22% to 57.67% in H358 cells (Table 2). These results suggest that OBP-301 is able to accumulate infected cells in S phase, which may render cells more sensitive to gemcitabine.

Changes in Cell Cycle Regulator Protein Expression following OBP-301 Infection

To clarify the mechanisms of cell cycle regulation by OBP-301, we analyzed the expression of proteins that have a crucial role in the cell cycle. H460, H322, and H358 cells were infected with OBP-301 at an MOI of 40, 100, and 80, and Western blot analysis was then done 24 hours later. As shown in Fig. 3B, expression levels of E2F1, as well as phosphorylated Akt, greatly increased after OBP-301 infection compared with the mock-infected controls in all three cell lines. p53 protein expression was not detectable in H460

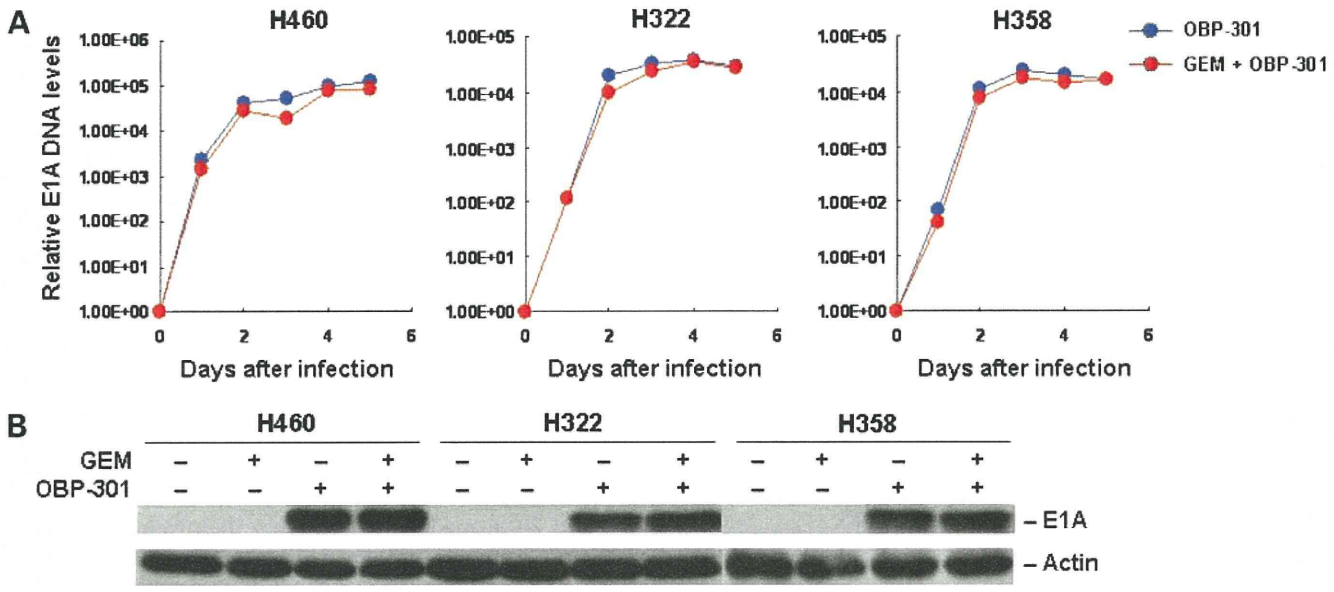

Figure 2. Assessment of viral DNA replication in human lung cancer cells. **A,** H460, H322, and H358 cells were infected with OBP-301 at an MOI of 10, 25, and 20, respectively, for 2 h as a baseline for virus DNA levels. Following the removal of virus inocula at 24 h after the infection, H460, H322, and H358 cells were further incubated with 70, 100, and 3 nmol/L of gemcitabine (*GEM*), respectively, for the indicated periods of time. Cells were then subjected to quantitative real-time PCR assay. Viral E1A copy number was defined as the fold increase for each sample relative to that at 2 h (2 h = 1). **B,** Western blot analysis of E1A expression in human lung cancer cells. Cells were treated with OBP-301, gemcitabine, or a combination of both, as described above, and then subjected to assay at 4 d after infection.

expressing the wild-type *p53* gene and p53-null H358 cells, whereas OBP-301 infection down-regulated mutant p53 expression in H322 cells.

Antitumor Effects of OBP-301 plus Gemcitabine in Human Lung Cancer Xenografts

Finally, we assessed the therapeutic efficacy of OBP-301 in combination with gemcitabine against H358 human lung cancer cells *in vivo*. H358 cells were implanted as xenografts into the hind flanks of *nu/nu* mice. Mice bearing palpable H358 tumors measuring 5 to 7 mm in diameter received simultaneous treatment of intratumoral injection of either 10^7 pfu OBP-301 or PBS plus i.p. administration of either 70 mg/kg gemcitabine or PBS every 3 days for three cycles starting at day 0. As shown in Fig. 4, administration of gemcitabine resulted in significant tumor growth suppression compared with mock-treated tumors for 34 days after initiation of treatment ($P < 0.05$); the combination of OBP-301 plus gemcitabine, however, produced a more profound and significant inhibition of tumor growth compared with mice treated with gemcitabine alone for at least 45 days ($P < 0.05$). The addition of OBP-301 clearly prolonged the antitumor effects of gemcitabine. Intratumoral injection of a replication-deficient adenovirus with or without systemic administration of gemcitabine had no apparent effect on the growth of H358 tumors (data not shown).

Discussion

Replication-competent oncolytic adenoviruses are promising as a novel anticancer therapy (9). In our laboratory, a tumor-specific replication-selective adenovirus, designated Telomelysin or OBP-301, is effective against human cancers (2–5). This virus was genetically designed to replicate under the control of hTERT promoter specifically in tumor cells, causing specific oncolysis. Despite the encouraging outcomes in animal experiments, combination chemotherapy and virotherapy are recommended in clinical treatment, as tumor progression is very rapid in most patients. In the current study, we explored the combination effects of OBP-301 and gemcitabine in human lung cancer cells *in vitro* and *in vivo*.

Adenovirus therapy combined with gemcitabine has been reported in the treatment of pancreatic cancer. Halloran et al. (9) reported that incubation of Panc-1 cells with either 5-fluorouracil or gemcitabine followed by adenovirus-mediated overexpression of $p16^{INK4A}$ resulted in a substantial reduction in cell viability under conditions where the drugs alone had minimal cytotoxicity. Although most studies reporting the combination effects of gemcitabine and adenoviral agents for pancreatic tumor used therapeutic genes critical for tumor growth inhibition, OBP-301 itself is an effective oncolytic virus and leads to infected cell destruction. Moreover, it has been reported that the type 5 adenoviral E1A sensitizes hepatocellular carcinoma cells to gemcitabine (10). These observations support the notion that oncolytic adenoviruses combined with gemcitabine are a rational modality for the treatment of human cancer.

The antitumor efficacy of OBP-301 was found to be enhanced when combined with gemcitabine in human lung cancer cells *in vitro* (Fig. 1; Table 1). Synergistic interaction was apparent in H460 and H358 cells; the combination

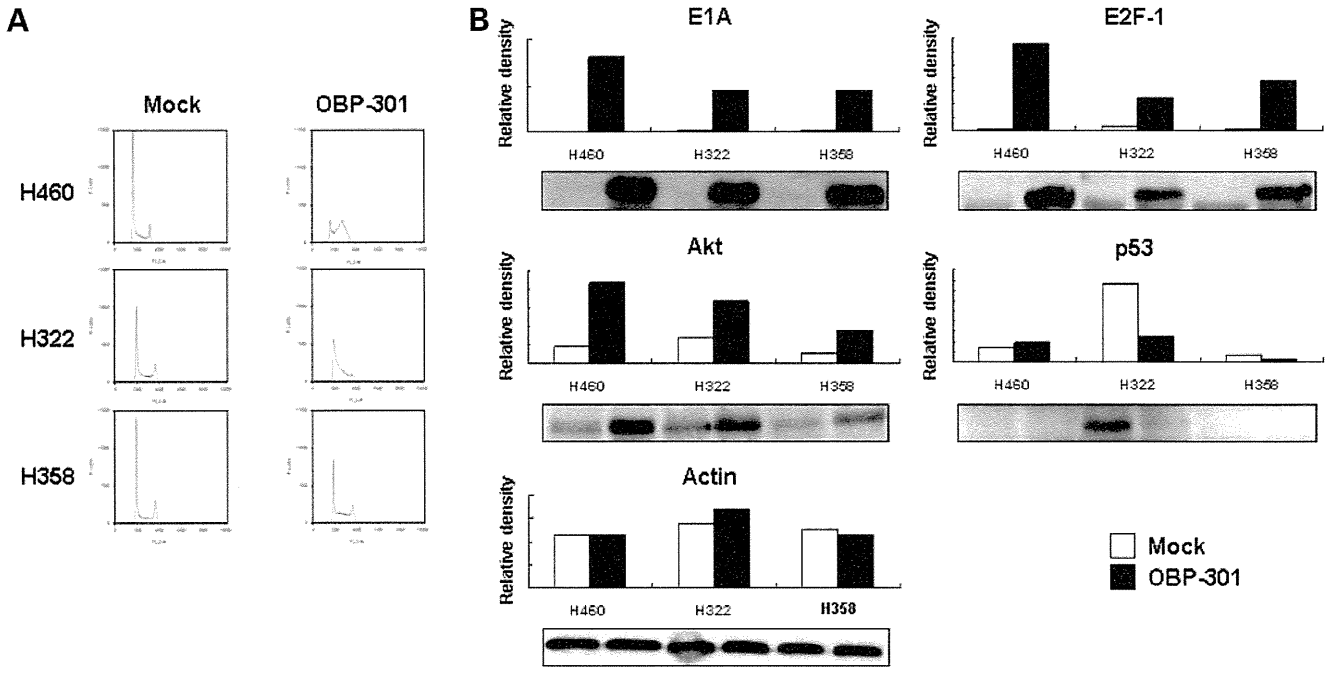

Figure 3. Cell cycle analysis and Western blotting of cell cycle regulator protein following OBP-301 infection in human lung cancer cells. **A,** H460, H322, and H358 cells were infected with OBP-301 at an MOI of 40, 100, and 80 MOI, respectively. DNA content was determined by propidium iodide staining and flow cytometric analysis at 24 h after OBP-301 infection. **B,** H460, H322, and H358 cells were either mock infected or infected with OBP-301 at an MOI of 40, 100, and 80 MOI, respectively. Following the removal of virus inocula, cells were collected at 24 h after infection and subjected to analysis. Equivalent amounts of protein obtained from whole-cell lysates were loaded into each lane, probed with primary antibodies, and then visualized using an enhanced chemiluminescence detection system. Equal loading of samples was confirmed by reprobing with antiactin antiserum. Protein expression was quantified by densitometric scanning using NIH Image software.

effect, however, was additive in H322 cells, suggesting that the effect of the combination is dependent on cell type. We also confirmed that this synergistic effect could be observed in human pancreatic cancer cells (Supplementary Fig. S3).[5] Gemcitabine is a deoxycytidine analogue and the incorporation of gemcitabine triphosphate into DNA causes chain termination, which is the major mechanism underlying the cytotoxicity of gemcitabine (11). Although there was concern over whether gemcitabine would interrupt the viral replication of OBP-301, quantitative real-time PCR analysis showed that intracellular replication of OBP-301 was not affected by gemcitabine (Fig. 2). The cytotoxic mechanisms of OBP-301 are distinct from those of gemcitabine, and therefore, combination effects could be observed provided that gemcitabine does not inhibit viral replication.

To clarify the mechanisms of the greater than additive response, cell cycle analysis was done following OBP-301 infection. Cells treated with OBP-301 tended to accumulate in the S phase at 24 hours after infection (Fig. 3A; Table 2). It has been reported that many DNA viruses can drive quiescent cells through G_1 into S phase by the expression of viral proteins (12–14). During the early phase of the adenovirus infection, the host cell is transformed into an efficient producer of the viral genome. The first gene that is transcribed in the viral genome is *E1A*, which can bind to numerous cellular proteins and acts as a multifunctional protein. Our data showed that OBP-301 infection increases the phosphorylation of Akt, as well as E2F1 expression, in all three human lung cancer cell lines (Fig. 3B). These effects are thought to be due to adenoviral E1A protein expression, as the dl312 adenovirus lacking the E1 genes did not phosphorylate Akt (data not shown).

Direct evidence of cell cycle promotion by Akt was seen when coexpression of Akt rescued cells from PTEN-induced cell cycle arrest (15). Retinoblastoma (Rb) protein restrains proliferation, in part, by modulating the activity of E2F

Table 2. Cell cycle analysis after OBP-301 infection in human lung cancer cells

Cell lines	Treatment	Cell cycle		
		G_1 (%)	S (%)	G_2 (%)
H460	Mock	43.54	43.85	8.61
	OBP-301	10.91	56.41	32.54
H322	Mock	40	46.72	10.85
	OBP-301	27.49	67.09	3.23
H358	Mock	45.89	38.22	14.29
	OBP-301	28.93	57.67	11.45

NOTE: H460, H322, and H358 cell lines were treated with OBP-301 at 40, 100, and 80 MOI, respectively. Cells were then subjected to cell cycle analysis at 24 h after treatment by the fluorescence-activated cell sorting method. The percentages of cells in the G_1, S, and G_2 phases are shown.

A

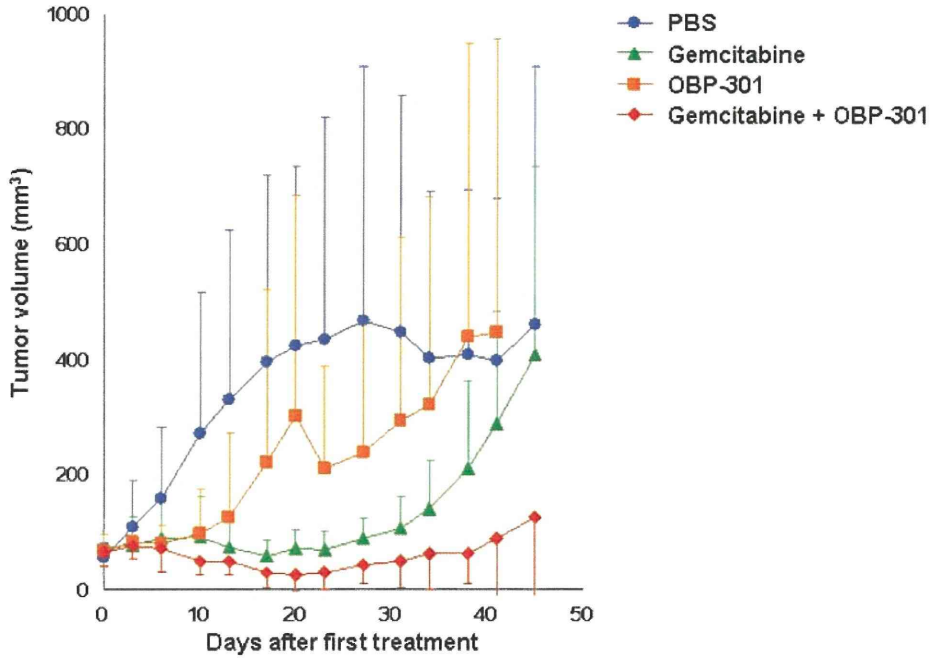

Figure 4. Antitumor effects of intratumorally injected OBP-301 and i.p. administered gemcitabine against established back H358 xenograft tumors in *nu/nu* mice. **A,** H358 tumor cells (5×10^6/each) were s.c. injected into the right flanks of mice. OBP-301 (1×10^8 pfu/body) and gemcitabine (70 mg/kg) were administered intratumorally and i.p., respectively, for three cycles every 3 d. PBS was used as the control. Eight mice were used for each group. Tumor growth is expressed as mean volume ± SE. **B,** statistical analysis was done using Student's *t* test for differences among indicated groups. Statistical significance (*red number*) was defined as $P < 0.05$.

B

	Day 23	Day 27	Day 31	Day 34	Day 38	Day 41	Day 45
PBS vs OBP-301	0.116	0.172	0.354	0.588	0.870	0.788	0.774
PBS vs Gemcitabine (GEM)	0.015	0.025	0.028	0.021	0.073	0.336	0.773
PBS vs GEM + OBP-301	0.009	0.014	0.014	0.005	0.004	0.008	0.051
OBP-301 vs GEM	0.034	0.068	0.101	0.155	0.198	0.377	0.594
OBP-301 vs OBP-301 + GEM	0.011	0.024	0.021	0.050	0.044	0.054	0.080
GEM vs OBP-301 + GEM	0.013	0.007	0.022	0.029	0.015	0.012	0.033

transcription factors. In quiescent cells, Rb associates with several E2Fs, resulting in the repression of proliferation-associated genes. As cells progress into the cell cycle, cyclin-dependent kinases phosphorylate Rb, freeing E2F and allowing it to directly transactivate genes required for S-phase entry (16). In fact, replication-deficient adenovirus-mediated *E2F1* gene transfer into human cancer cells resulted in accumulation of an S-phase cell population (Supplementary Fig. S4).[5] Thus, OBP-301 infection expressed E1A protein, which in turn up-regulated the expression of phosphorylated Akt and E2F1, leading to cell cycle promotion and S-phase entry presumably by the deactivation of Rb. Indeed, we confirmed that OBP-301 infection decreased Rb protein expression in H460 cells (data not shown). The accumulation of the tumor cells in S phase increases the cytotoxicity of gemcitabine, which kills cells in S phase.

In summary, our data show that telomerase-specific oncolytic adenovirus infection increases the sensitivity of human lung cancer cells to gemcitabine due to S-phase accumulation. The combination of OBP-301 and gemcitabine efficiently inhibits human cancer cell growth both *in vitro* and *in vivo*, an outcome that has important implications for tumor-specific oncolytic chemovirotherapies for human lung cancer.

Disclosure of Potential Conflicts of Interest

M. Ouchi, H. Onimatsu, and Y. Urata: employees of Oncolys BioPharma, Inc. T. Fujiwara: consultant for Oncolys BioPharma, Inc. No other potential conflicts of interest were disclosed.

Acknowledgments

We thank Daiju Ichimaru and Hitoshi Kawamura for their helpful discussions and Tomoko Sueishi for her excellent technical support.

References

1. Gkiozos I, Charpidou A, Syrigos K. Developments in the treatment of non-small cell lung cancer. Anticancer Res 2007;27:2823–7.

2. Kawashima T, Kagawa S, Kobayashi N, et al. Telomerase-specific replication-selective virotherapy for human cancer. Clin Cancer Res 2004;10:285–92.

3. Taki M, Kagawa S, Nishizaki M, et al. Enhanced oncolysis by a tropism-modified telomerase-specific replication-selective adenoviral agent OBP-405 ('Telomelysin-RGD'). Oncogene 2005;24:3130–40.

4. Hashimoto Y, Watanabe Y, Shirakiya Y, et al. Establishment of biological and pharmacokinetic assays of telomerase-specific replication-selective adenovirus. Cancer Sci 2008;99:385–90.

5. Endo Y, Sakai R, Ouchi M, et al. Virus-mediated oncolysis induces danger signal and stimulates cytotoxic T-lymphocyte activity via proteasome activator upregulation. Oncogene 2008;27:2375–81.

6. Khuri FR, Nemunaitis J, Ganly I, et al. A controlled trial of intratumoral ONYX-015, a selectively-replicating adenovirus, in combination with cisplatin and 5-fluorouracil in patients with recurrent head and neck cancer. Nat Med 2000;6:879–85.

7. Paz-Ares L, Douillard JY, Koralewski P, et al. Phase III study of gemcitabine and cisplatin with or without aprinocarsen, a protein kinase C-α antisense oligonucleotide, in patients with advanced-stage non-small-cell lung cancer. J Clin Oncol 2006;24:1428–34.

8. Heinemann V, Quietzsch D, Gieseler F, et al. Randomized phase III trial of gemcitabine plus cisplatin compared with gemcitabine alone in advanced pancreatic cancer. J Clin Oncol 2006;24:3946–52.

9. Halloran CM, Ghaneh P, Shore S, et al. 5-Fluorouracil or gemcitabine combined with adenoviral-mediated reintroduction of p16INK4A greatly enhanced cytotoxicity in Panc-1 pancreatic adenocarcinoma cells. J Gene Med 2004;6:514–25.

10. Lee WP, Tai DI, Tsai SL, et al. Adenovirus type 5 E1A sensitizes hepatocellular carcinoma cells to gemcitabine. Cancer Res 2003;63:6229–36.

11. Huang P, Chubb S, Hertel LW, Grindey GB, Plunkett W. Action of 2',2-difluorodeoxycytidine on DNA synthesis. Cancer Res 1991;51:6110–7.

12. Wang HG, Draetta G, Moran E. E1A induces phosphorylation of the retinoblastoma protein independently of direct physical association between the E1A and retinoblastoma products. Mol Cell Biol 1991;11:4253–65.

13. Hollyoake M, Stühler A, Farrell P, Gordon J, Sinclair A. The normal cell cycle activation program is exploited during the infection of quiescent B lymphocytes by Epstein-Barr virus. Cancer Res 1995;55:4784–7.

14. Morozov A, Shiyanov P, Barr E, Leiden JM, Raychaudhuri P. Accumulation of human papillomavirus type 16 E7 protein bypasses G_1 arrest induced by serum deprivation and by the cell cycle inhibitor p21. J Virol 1997;71:3451–7.

15. Paramio JM, Navarro M, Segrelles C, Gomez-Casero E, Jorcano JL. PTEN tumor suppressor is linked to the cell-cycle control through the retinoblastoma protein. Oncogen 1999;18:7462–8.

16. Nahle Z, Polakoff J, Davuluri RV, et al. Direct coupling of the cell cycle and cell death machinery by E2F. Nat Cell Biol 2002;4:859–64.

In vivo internal tumor illumination by telomerase-dependent adenoviral GFP for precise surgical navigation

Hiroyuki Kishimoto[a,b,c], Ming Zhao[a], Katsuhiro Hayashi[a,b], Yasuo Urata[d], Noriaki Tanaka[c], Toshiyoshi Fujiwara[c,e], Sheldon Penman[f,1], and Robert M. Hoffman[a,b,1]

[a]AntiCancer, Inc., San Diego, CA 92111; [b]Department of Surgery, University of California, San Diego, CA 92103-8220; [c]Division of Surgical Oncology, Department of Surgery, Okayama University Graduate School of Medicine, Dentistry and Pharmaceutical Sciences, Okayama 700-8558, Japan; [d]Oncolys BioPharma, Inc., Tokyo 106-0032, Japan; [e]Center for Gene and Cell Therapy, Okayama University Hospital, Okayama 700-8558, Japan; and [f]Department of Biology, Massachusetts Institute of Technology, Cambridge, MA 02139-4307

Contributed by Sheldon Penman, June 8, 2009 (sent for review May 10, 2009)

Cancer surgery requires the complete and precise identification of malignant tissue margins including the smallest disseminated lesions. Internal green fluorescent protein (GFP) fluorescence can intensely illuminate even single cells but requires *GFP* sequence transcription within the cell. Introducing and selectively activating the *GFP* gene in malignant tissue in vivo is made possible by the development of OBP-401, a telomerase-dependent, replication-competent adenovirus expressing GFP. This potentially powerful adjunct to surgical navigation was demonstrated in 2 nude mouse models that represent difficult surgical challenges—the resection of widely disseminated cancer. HCT-116, a model of intraperitoneal disseminated human colon cancer, was labeled by virus injection into the peritoneal cavity. A549, a model of pleural dissemination of human lung cancer, was labeled by virus administered into the pleural cavity. Only the malignant tissue fluoresced brightly in both models. In the intraperitoneal model of disseminated cancer, fluorescence-guided surgery enabled resection of all tumor nodules labeled with GFP by OBP-401. The data in this report suggest that adenoviral-GFP labeling tumors in patients can enable fluorescence-guided surgical navigation.

Adenovirus | green fluorescent protein | metastasis

The intent of cancer surgery is to remove malignant tissue together with margins of presumably normal tissue (1–3) to ensure complete removal of abnormal cells. Estimating margin width during surgery is critical and depends on the surgeon's vision. There have been many developments intended to improve the delineation of tissue margins using morphologic and optical differences between normal and abnormal tissue. This report describes a major enhancement of cancer surgical navigation using the selective fluorescent labeling, in vivo, of malignant tissue. Bright GFP fluorescence clearly illuminates the tumor boundaries and facilitates detection of the smallest disseminated disease lesions.

Highly selective viral replication in malignant cells growing in normal tissue has recently become possible using novel adenoviruses, OBP-301 (4–6) and, more recently, OBP-401 (7, 8). This latter virus, which can enter most cells, contains the replication cassette with the human telomerase reverse transcriptase (hTERT) promoter driving the expression of the viral *E1* genes, and the inserted *GFP* gene. Virus replication and, hence, *GFP* gene expression occur only in the presence of an active telomerase, i.e., in malignant tissue (7). The OBP-401 virus was first tested by injection directly into HT-29 human colon tumors orthotopically implanted into the rectum in BALB/c *nu/nu* mice (7). Subsequent para-aortic lymph node metastasis was observed by laparotomy under fluorescence. The adaption of GFP fluorescence to in vivo labeling of tumor tissue should facilitate precision surgical navigation in live animals and, very possibly, in a clinical surgical setting.

Results

Fluorescence Labeling of Human Cancer Cells with OBP-401 in Vitro. A549 tumor cells, growing in tissue culture, were infected with OPP-401, and the development of GFP fluorescence followed. The fluorescence intensity gradually increased after infection as the virus, with its *GFP* gene, replicated (Fig. 1*A*).

The extent of infection was tested by infecting red fluorescent protein (RFP)-expressing cancer cells, growing in cell culture, with OBP-401. These included A549-RFP, PC-3-RFP, HCT-116-RFP, and HT-29-RFP cells. In most cells, the introduction of green fluorescence changes the cell color from red to yellow, showing that most were infected by OBP-401. Any remaining red fluorescence clearly identifies those few cells that remain uninfected by the adenovirus. The color changes increased gradually followed by cell death due to the cytopathic effect of replicating OBP-401 (Fig. 1 *B* and *C*).

Fluorescence Labeling of Subcutaneous Tumors by Infection in Vivo with OBP-401. Both nonfluorescent PC-3 and red fluorescent PC-3-RFP human prostate cancer cells were inoculated s.c. (Fig. 2 *A* and *B*). The resulting s.c. tumors were injected with 1×10^8 plaque-forming units (PFU) of OBP-401 as shown in Fig. 2*B*. A color change from red to yellow in the s.c. PC-3-RFP tumor and the onset of GFP fluorescence in the nonfluorescent PC-3 tumor were observed by the third day after virus injection (Fig. 2*C*). An RFP filter selectively showed the tumors' endogenous RFP fluorescence (Fig. 2*D*). Similarly, a GFP filter showed GFP fluorescence induced in the tumors by OBP-401 (Fig. 2*E*). Infecting tumor cells that are endogenously expressing RFP with the GFP-expressing adenoviral vector OBP-401 clearly shows the extent of GFP labeling of the tumor. Cells showing a yellow fluorescence are infected with OBP-401, while the remaining red fluorescent cells clearly indicate the small portion that might remain uninfected.

Labeling Peritoneal Carcinomatosis with OBP-401. Peritoneal carcinomatosis was induced in the abdominal cavity of nude mice by inoculating 3×10^6 red fluorescent HCT-116-RFP human colorectal cancer cells. Various sized peritoneal disseminated nodules developed within 12 days. These were clearly visible by fluorescence imaging using a long-pass filter and/or a specific RFP filter (Fig. 3 *A* and *B*). Even very small disseminated nodules were illuminated by RFP fluorescence (Fig. 3*B*). Although there was some autofluorescence from adjacent organs visible, the tumor nodules were not visible through a GFP filter (Fig. 3 *A* and *B*).

Author contributions: H.K., Y.U., N.T., T.F., and R.M.H. designed research; H.K., M.Z., and K.H. performed research; H.K., Y.U., N.T., T.F., S.P., and R.M.H. analyzed data; and H.K., S.P., and R.M.H. wrote the paper.

The authors declare no conflict of interest.

[1]To whom correspondence may be addressed. E-mail: penman@mit.edu or all@anticancer.com.

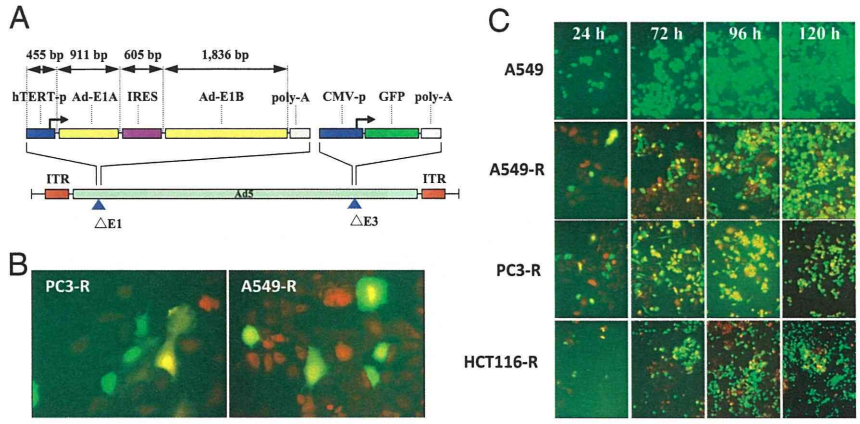

Fig. 1. Structure of OBP-401, virus replication in human cancer cells and induced GFP expression. (*A*) Schematic DNA structure of OBP-401. OBP-401 is a telomerase-specific replication-competent adenovirus variant, in which the hTERT promoter element drives the expression of *E1A* and *E1B* genes linked with an IRES. The *GFP* gene is inserted under the CMV promoter into the E3 region. (*B*) A549-RFP and PC-3-RFP cells changed color after infection with OBP-401 at a multiplicity of injection (MOI) of 10. (Magnification, 200×.) (*C*) Noncolored A549 as well as RFP-expressing cancer cells A549-RFP, PC-3-RFP, and HCT-116-RFP were infected with OBP-401 at an MOI of 10. Cells were assessed at indicated time points for GFP expression under fluorescence microscopy. After OBP-401 infection, noncolored A549 cells expressed GFP fluorescence. In A549-RFP, PC-3-RFP, and HCT-116-RFP, color changes from red to yellow were detected. The color changes increased gradually in a time-dependent fashion. (Magnification, 200×.)

Once the malignant nodules were established at 12 days after intraperitoneal (i.p.) implantation of HCT-116-RFP cells, 1×10^8 PFU OBP-401 were injected into the mouse abdominal cavity. Selective color filters showed that the HCT-116-RFP disseminated nodules expressed GFP fluorescence as well as RFP when examined 5 days later (Fig. 3*C*). RFP fluorescence

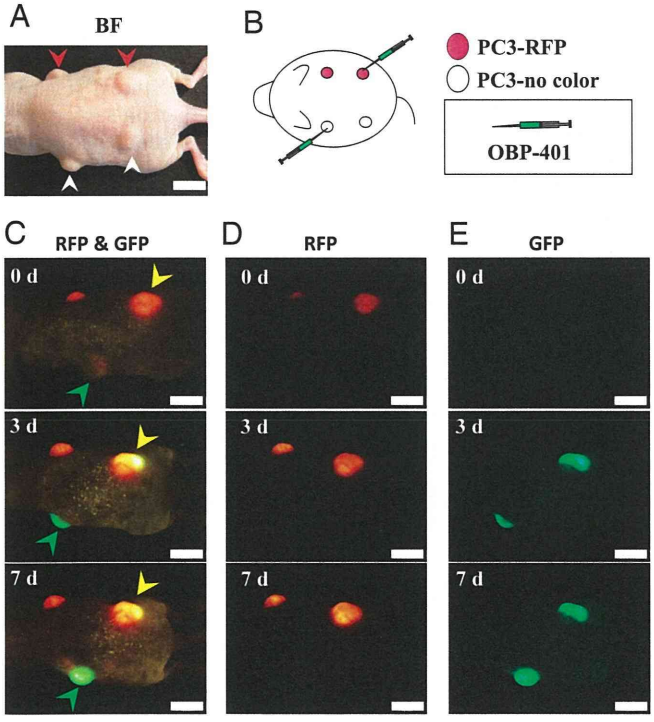

Fig. 2. Selective visualization of s.c. tumors in vivo after OBP-401 GFP-labeling. s.c. tumors of noncolored PC-3 (*A*, white arrowheads) or PC-3-RFP (*A*, red arrowheads) human prostate cancer cells were intratumorally injected with PBS for control or OBP-401 at a dose of 1×10^8 PFU as shown in *B*. After intratumoral injection of OBP-401, GFP fluorescence was detected in noncolored PC-3 s.c. tumors (*C*, green arrowheads) and a color change from red to yellow was also observed in PC-3-RFP tumors by fluorescence imaging using a long-pass filter to simultaneously observe both GFP and RFP (*C*, yellow arrowheads). With specific filters, the tumors endogenous RFP fluorescence (*D*) and GFP fluorescence induced by OBP-401 (*E*) were individually detected. (Scale bar, 10 mm.)

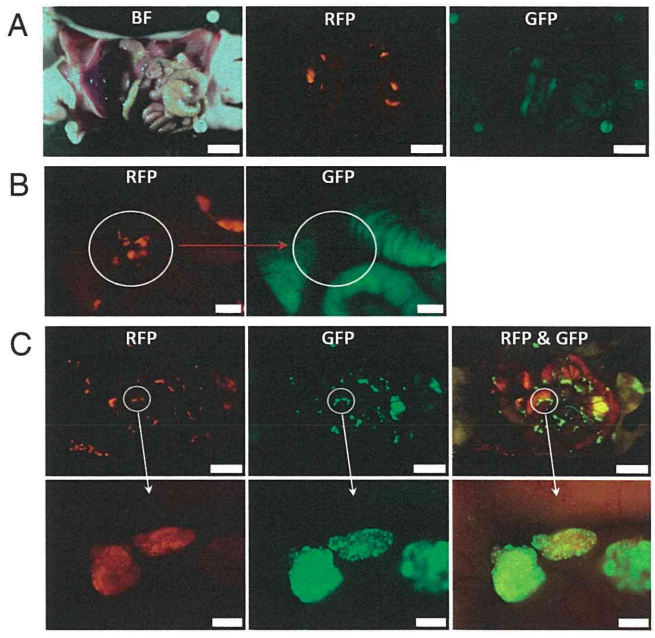

Fig. 3. Intraperitoneal injection of OBP-401 visualized peritoneal dissemination of HCT-116-RFP cells. (*A*) HCT-116-RFP human colorectal cancer cells were inoculated into the abdominal cavity of nude mice. Various sized disseminated peritoneal nodules appeared within 12 days. (Scale bar, 10 mm.) (*B*) At higher magnification, peritoneally disseminated nodules of HCT-116-RFP were clearly visible using a specific filter for RFP (*Left*), and these nodules did not express GFP (*Right*). (Scale bar, 2 mm.) (*C*) Mice with HCT-116-RFP peritoneal disseminated nodules were i.p. injected with OBP-401 at a dose of 1×10^8 PFU. Five days after virus administration, HCT-116-RFP peritoneal-disseminated nodules were detected with their endogenous RFP fluorescence (*Left*). These disseminated nodules now expressed GFP fluorescence (*Middle*). With the long-pass filter, for simultaneous observation of both GFP and RFP, it can be seen that all of the RFP tumors were apparently labeled with GFP after OBP-401 injection (*Right*). (Scale bars: *Upper*, 10 mm; *Lower*, 500 μm.)